REVIEW

Plasmonic Nanolasers

www.advopticalmat.de

ADVANCED
OPTICAL
MATERIALS

Plasmonic Nanolasers: Pursuing Extreme Lasing Conditions on Nanoscale

Hao Wu, Yixiao Gao, Peizhen Xu, Xin Guo,* Pan Wang, Daoxin Dai, and Limin Tong*

Owing to their ultrahigh optical confinement, plasmonic nanolasers with cavity sizes beyond the diffraction limit of light, are attracting increasing attention for pursuing extreme lasing conditions on nanoscale including ultracompact cavity mode, ultrafast lasing modulation, significantly enhanced light–matter interaction, and Purcell effect. In this review, the recent progress on plasmonic nanolasers from both theoretical and experimental aspects is introduced, with emphases on plasmonic nanolasers with subdiffraction-limit cavity-mode confinement. Starting from a theoretical model and key parameters of a plasmonic nanolaser, general concerns of materials for both plasmonic cavities and gain media are summarized. Then, experimental efforts on realization of plasmonic nanolasers with cavity-mode confinement increased from 1 to 3 dimensions are reviewed, followed by a brief introduction of some novel designs of plasmonic nanolasers and plasmon-assisted nanolasers. Finally, future prospects and challenges in pursuing extreme lasing conditions of plasmonic nanolasers are discussed, and the identification of lasing threshold in these tiny lasers is revisited.

1. Introduction

As a highly directional and coherent light source, laser is light amplification by stimulated emission of radiation in a cavity.[1] Since its invention in 1960,[2] laser has been playing crucial roles in a variety of human activities ranging from scientific research to daily life. In past decades, the rapid evolutions of laser technology, as well as the growing demands for laser applications including nuclear fusion,[3] ultrafast spectroscopy,[4–7] and on-chip optical network,[8–10] have been the driving force for developing lasers with higher peak power, shorter pulse duration, smaller cavity size, and broader spectral range, along which a number of novel laser mechanisms, designs,

and techniques have been proposed and/or developed. Here we focus on a newly emerging area—plasmonic nanolaser that pursuing extremely smaller cavity size in one or more dimensions, and consequently extreme lasing conditions, by using a plasmonic cavity with feature size possibly far below the diffraction limit of light.

The miniaturization of a laser can be traced back to the early age of the laser, when compact semiconductor structures were introduced. In particular, the introduction of semiconductors as the gain media in 1962,[11,12] followed by a series of elaborately engineered structures from heterostructure,[13] quantum well,[14] vertical-cavity surface-emitting laser (VCSEL),[15,16] microdisk,[17–19] photonic crystal,[20–22] quantum dot[23,24] to nanowire (NW)[25–27] have made great success in shrinking a laser from bulk scale to wavelength level using reduced cavity sizes.[28] For example, to date, typical commercial edge-emitting quantum well laser diodes have dimensions of several micrometers in width and hundreds of micrometers in length, and a single quantum dot can lase in a photonic crystal cavity with overall dimension of merely $0.7(\lambda/n)^3$, where λ is the vacuum wavelength and n the refractive index of the dielectric.[29] With optimized geometry and material for cavity design, lower structural dimension is expected. However, in a dielectric cavity with limited refractive index n, the cavity size is intrinsically restricted by optical diffraction limit that sets an ultimate limit $\lambda/2n$ for both cavity length and mode size in all three dimensions.

An effective step to shrink a cavity beyond the diffraction limit is converting light into surface plasmon polaritons (SPPs) in nanostructuralized metals, which is a kind of collective oscillation of quasi free electrons on the interface of a metal and a dielectric.[30] While SPP is featured with ultrahigh optical confinement and ultrafast relaxation process as shown in **Figure 1**a,[31] it is inevitably accompanied by ultrahigh energy dissipation (i.e., Ohmic loss), leading to a mutual balance between the mode size and the optical loss in either a nanowaveguide or a nanocavity as shown in Figure 1b.[32] For example, the transverse mode area of SPP mode on an Ag nanowire with diameter of 100 nm can be as small as $0.01~\mu m^2$ but also exhibits a propagation loss larger than 200 dB mm^{-1}. Despite of the high loss coefficient of plasmonic resonance at optical frequency, a properly designed nanoplasmonic cavity coupled with a gain medium is possible to lase with miniature cavity length.

H. Wu, Dr. Y. X. Gao, P. Z. Xu, Prof. X. Guo, Dr. P. Wang, Prof. D. X. Dai, Prof. L. M. Tong
State Key Laboratory of Modern Optical Instrumentation
College of Optical Science and Engineering
Zhejiang University
Hangzhou 310027, China
E-mail: guoxin@zju.edu.cn; phytong@zju.edu.cn
Prof. L. M. Tong
Collaborative Innovation Center of Extreme Optics
Shanxi University
Taiyuan 030006, China

The ORCID identification number(s) for the author(s) of this article can be found under https://doi.org/10.1002/adom.201900334.

ADVANCED
SCIENCE NEWS
www.advancedsciencenews.com

ADVANCED
OPTICAL
MATERIALS
www.advopticalmat.de

In 2003, Bergman and Stockman proposed the concept of surface plasmon amplification by stimulated emission of radiation (SPASER) with a plasmonic feedback cavity, whose size is possibly to be reduced far below the diffraction limit of light in vacuum.[33] Later in 2009, plasmonic lasers with mode sizes well below the diffraction limit was reported experimentally,[34,35] which soon attracted broad attentions from nanophotonics, plasmonics to laser communities.[36–53] Compared to a conventional "photonic nanolaser" relying on a dielectric cavity with feature size (cavity or mode size) equal to or larger than $\lambda/2n$, a plasmonic nanolaser offers an opportunity to reduce the mode size smaller than $\lambda/20$, whereas n is usually smaller than 5 for dielectrics at low-absorption frequency. The ultratight confinement of optical fields in a nanoplasmonic cavity brings unique situations for pursuing extreme lasing conditions including ultracompact cavity mode, ultrafast lasing modulation, significantly enhanced light–matter interaction and Purcell effect, which in turn brings new frontiers of laser science and technology, as well as arguments to revisit the lasing criterions on the new scale.

In this paper, we review recent progresses in this field, with emphases on plasmonic nanolasers with subdiffraction-limit cavity modes. Starting from a theoretical model of a SPASER, we review the principles and key parameters of a plasmonic nanolaser, followed by general concerns of materials for both plasmonic cavities and gain media. Then, we review experimental efforts on realization of plasmonic nanolasers with cavity-mode confinement increased from 1 to 3 dimensions. A fraction of novel designs of plasmonic nanolasers and some typical plasmon-assisted nanolasers are also briefly mentioned. Finally, we discuss future prospects and challenges in pursuing extreme lasing conditions of plasmonic nanolasers, and revisit the identification of lasing threshold in these tiny lasers.

2. Theoretical Model of a Plasmonic Laser

Generally, a plasmonic laser consists of three parts: an active material to provide the gain, a plasmonic cavity to provide the feedback, and a pumping source to provide the excitation. A typical laser configuration is schematically illustrated in **Figure 2**, in which the gain material is a three-level emitter (e.g., a semiconductor quantum dot or an organic dye molecule), the cavity feedback is provided by a propagation or localized plasmonic mode, and the pumping energy can be provided either electronically or optically. The interaction strength between the emitter and the cavity is denoted as Ω_R. The excited level is assumed to experience a homogeneous broadening with inherent damping rate γ_e, and the cavity has a damping rate γ_p.

When such a lasing system operates in the weak-coupling regime, i.e., $\Omega_R < |\gamma_e - \gamma_p|/2$, it can be basically described by a single-mode rate equation, expressing as two coupled ordinary differential equations of the excited carrier number N and photon number s in the cavity mode[38]

$$\frac{dN}{dt} = R - \Gamma F_p \beta_0 A (N - N_{tr}) s - \Gamma F_p \beta_0 A N - \frac{N}{\tau_{nr}} \tag{1a}$$

$$\frac{ds}{dt} = \Gamma F_p \beta_0 A (N - N_{tr}) s + \Gamma F_p \beta_0 A N - \gamma_p s \tag{1b}$$
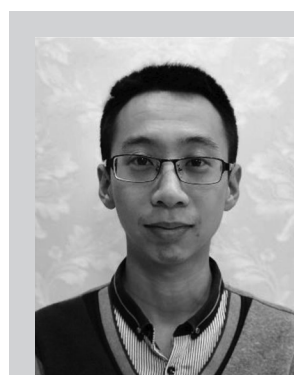
Hao Wu is a Ph.D. candidate of the College of Optical Science and Engineering at Zhejiang University, China, under the supervision of Prof. Limin Tong. He received his B.Sc. in Information Engineering from Tianjin University in 2016. His current research focuses on plasmonic lasers and nanophotonics.

Xin Guo is an associate professor of the College of Optical Science and Engineering at Zhejiang University, China. She received a B.S. degree in Optical Information Science and Technology from Sichuan University in 2005 and a Ph.D. degree in Optical Engineering from Zhejiang University in China in 2010. Her current research interests include nanophotonics and plasmonics.

Limin Tong received his Ph.D. from Zhejiang University in 1997. He is currently a professor of the College of Optical Science and Engineering at Zhejiang University, China. His main research interests include nanophotonics, nanoplasmonics, and fiber optics, with emphases on nanowaveguides and nanophotonic devices. He is fellow of the OSA, and an associate editor of Optica.

where R is the pump rate, Γ is the confinement factor, F_p is the Purcell factor, β_0 is the fraction of the spontaneous emission photon into the lasing mode without the Purcell effect, A is the spontaneous emission rate, N_{tr} is the transparent excited carrier density, and τ_{nr} is the nonradiative transition lifetime.

More specifically, the confinement factor Γ, taking a value between [0, 1], is defined as the density overlap between the excited carriers and the cavity mode energy, and can be obtained as

$$\Gamma = \int \tilde{N}(r)\tilde{s}(r)\,dV \tag{2}$$

**ADVANCED
SCIENCE NEWS**
www.advancedsciencenews.com

**ADVANCED
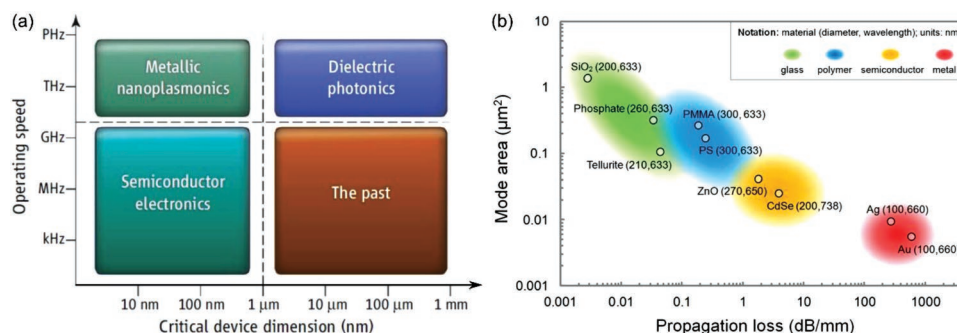OPTICAL
MATERIALS**
www.advopticalmat.de

Figure 1. Primary pros and cons of manipulating light with nanoplasmonics. a) Unique material properties of semiconductors (electronics), dielectrics (photonics), and metals (plasmonics) for device applications in terms of operating speed and critical size. The dashed lines indicate physical limitations of different technologies. b) Trade-off between mode sizes and optical losses of nanowire waveguides made of different materials. a) Reproduced with permission.[31] Copyright 2010, American Association for the Advancement of Science. b) Reproduced with permission.[32] Copyright 2013, American Chemical Society.

where $\tilde{N}(r)$ is position-dependent normalized excited carrier density with $\int \tilde{N}(r)\,dV = 1$ and $\tilde{s}(r)$ the position-dependent normalized mode energy density of cavity mode with $\max\{\tilde{s}(r)\} = 1$ and $\int \tilde{s}(r)\,dV = V_{\text{eff}}$.[54]

Equation (1a) determines the time-dependent population of the excited carriers, where the first term R represents the pump rate, the second and third term represent losses due to stimulated and spontaneous emissions to lasing mode, respectively, and the last term represents loss due to nonradiative recombination. Equation (1b) determines the time-dependent population of the polaritons, where the first two terms represent

the generated population due to stimulated and spontaneous emission, respectively, and the last term represents the loss from the cavity.

Compared with a conventional laser using a photonic cavity, a plasmonic laser with extreme confinement described by Equation (1) should consider more factors that may play important roles in lasing behavior, as we summarized below.

2.1. Purcell Effect

Within weak coupling regime, when the spectral width of the cavity resonance is broader than that of the emitter inside, Purcell effect can be evaluated by the Purcell factor using Fermi's golden rule[55]

$$F_{\text{p}} = \frac{3}{4\pi^2} \frac{Q}{V_{\text{eff}}} \left(\frac{\lambda}{n}\right)^3 \tag{3}$$

which quantifies the enhancement of the emission rate into a specific mode in a modified electromagnetic environment relative to that into the vacuum. Here, V_{eff} is the effective cavity mode volume, Q is the quality factor of the cavity, and n is refractive index of background dielectric environment.

In bulk laser systems, Purcell effect is usually neglectable due to the large V_{eff}. However, it becomes evidently large in microcavities with a small V_{eff} and a relatively large Q, as have been reported in microcavity nanolasers.[56] Compared with a photonic cavity, a plasmonic laser cavity typically has a much lower Q. However, the plasmonic cavity size V_{eff} can also be much smaller, resulting in evident Purcell effect measured by Q/V_{eff}, as have been experimentally observed in plasmonic nanolasers.[57–59] The large Purcell factor of the lasing mode leads to a larger spontaneous emission factor β than the original β_0, which may be helpful for reducing the lasing threshold. Genov et al. studied the Purcell factor of an emitter placed in close proximity to plasmonic systems with 1D and 2D confinement, where the propagating SPPs are confined on a 2D surface or along a quasi 1D wire, as shown in **Figure 3**a.[60] The introduction of the feedback, as the case of a laser, further enhances the spontaneous emission rate of the emitter
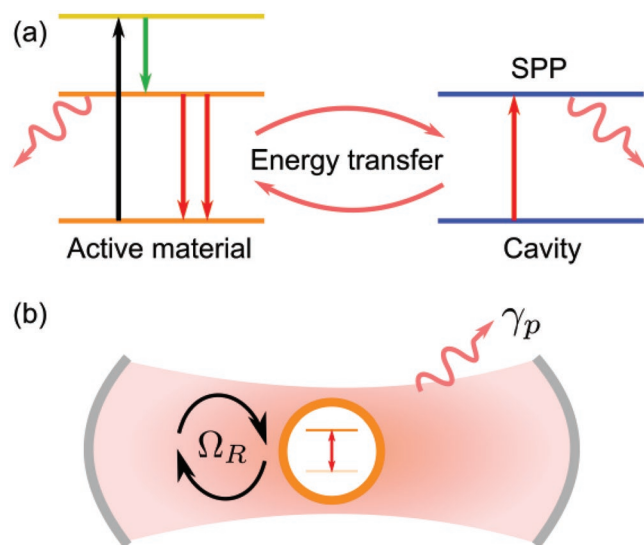

Figure 2. Schematic illustration of a plasmonic nanolaser. a) The external pump excites the active material to a high excited level (black arrow), which transits to a metastable state via fast relaxation (green arrow) to form an exciton. The exciton recombines and transits to ground state via either radiative (red straight arrows) or nonradiative (red waved arrow) transitions and exchanges energy with plasmonic cavity mode. The cavity mode interacts with excitons at excited states to trigger stimulated emission and generate lasing oscillation (red curve arrows) with a certain degree of cavity loss (red waved arrow). b) Diagrams of the interaction strength Ω_R between the emitter and the cavity, and the energy dissipates rate γ_p of the cavity mode.
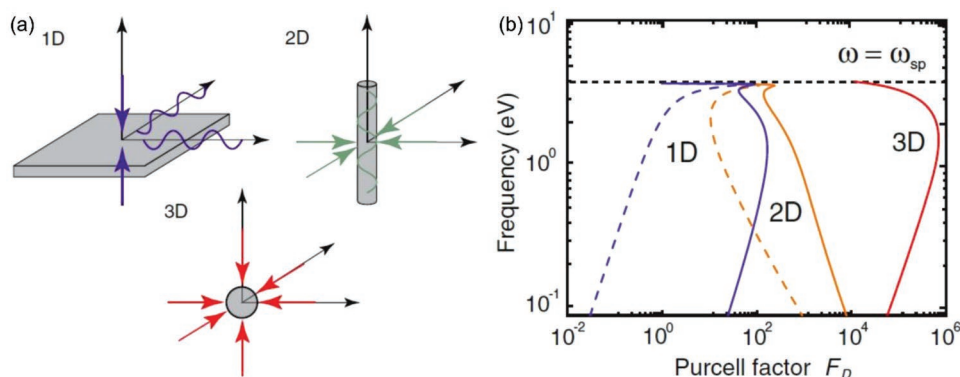
Figure 3. Purcell effects in 1D-, 2D-, and 3D-confined nanostructures. a) Schematic diagram of metal nanostructures supporting SPP modes. b) Frequency-dependent Purcell effects of emitters coupled to SPPs supported by the 1D- (planar silver/air interface), 2D- (40 nm diameter silver nanowire in air), and 3D- (nanosize silver particle in air) confined structures, respectively. The plots are divided into intrinsic (broken lines) and cavity-enhanced (solid lines) enhancement factors, where feedback has been introduced through cavity mirrors in a Fabry–Perot configuration with longitudinal mode order of 1 and end-facet reflectivity of 0.99. The red solid line shows the limits of plasmonics where nonlocal effects become significant, which could be reached with metallic nanoparticle SP resonators. Reproduced with permission.[60] Copyright 2011, American Physical Society.

proportional to the cavity finesse in 1D and 2D systems. Additional enhancement of the Purcell factor can also be observed near the surface plasmon frequency. The metallic nanoparticles, which achieve confinement in all three dimensions, are the smallest possible plasmonic cavities limited by the nonlocal effects. Figure 3b presents the attainable Purcell effect in nanoparticles before the nonlocal effects emphasize. Though the metallic nanoparticles exhibit the highest Purcell factor, in this occasion, loss of these localized surface plasmonic mode is expected to increase drastically.

With enhanced coupling strength, the emitter-cavity system will enter into strong-coupling regime, where $\Omega_R > |\gamma_e - \gamma_p|/2$. In this regime, excitons in the active materials and polaritons in the cavity mode cannot be distinguished and a new kind of quasiparticle called exciton–polariton will emerge.[61] As a result of its boson nature, polariton Bose condensation can be achieved to emit coherent light that is sometimes called polariton laser, but with a different mechanism from a conventional laser.[55] Polariton lasers have been achieved in some VCSEL devices,[62–65] and have been observed in plasmonic system more recently.[66]

2.2. Nonradiative Channels

In a laser working in steady state, the excited atoms or molecules at upper levels are expected to return to lower levels by radiating photons into lasing modes via stimulated or spontaneous emission. However, the upper level population can also be depleted via nonradiative channels, which may be originated from the gain material itself (e.g., Auger recombination caused by phonon collision[38]) or other associated effects (e.g., surface recombination due to surface defects[67]). The introduction of plasmonic structures may offer new channels for nonradiative transition. Besides the enhancement of the emission rate, the coupling between the emitter and the plasmonic system may also enhance the transition rate of the emitter to some undesirable near-field nonradiative channels in forms of, e.g., high-order modes of the metallic nanoparticles,[68]

lossy surface modes, and electron–hole excitations in the metal.[69–71] Nonradiative transition through these channels, although becomes evident only in the near field, increases with decreasing spacing between the emitter and the plasmonic structure, can be pronounced when the spacing is reduced to nanometer level. With the possibly large enhancement of the nonradiative-channel damping rate, the far-field emission from the emitter will be seriously suppressed, and this kind of quenching phenomenon has been theoretically predicted[68,69,72] and experimentally observed[70,71,73] in nanoplasmonic systems. Therefore, to avoid such quenching effect in plasmonic nanolasers, an insulator nanospacer between the gain materials and plasmonic structures is recommended.[35]

2.3. Lasing Threshold

Conventional definition of the lasing threshold is the pumping density where the pump-dependent gain equals the cavity loss. Experimentally, the threshold is usually obtained at the "turning" point on the pump–output curve, where the fractions of stimulated emission is assumed equal to that of the spontaneous emission. In a nanolaser with a considerably large Purcell factor, β could also be large to smear the "turning" behavior, making it difficult to identify the threshold. What's more, in a laser with $\beta \approx 1$, there is no "turning" point, which is sometimes termed as a "thresholdless" laser, although in principle, the cavity mode of enhanced spontaneous emission is fundamentally different with that of stimulated emission in phase, coherence, and photon statistics.[74] To clarify the lasing threshold, stricter definitions are proposed based on the coherence nature,[75,76] among which a widely accepted criterion is given as[76] the point where the stimulated emission rate is equal to the spontaneous emission rate. At this pump level, the mean photon number in the lasing mode at threshold is unity, i.e., $s_{th} = 1$. Thus the threshold can be derived as (neglecting the nonradiative term)[77]

$$R_{th} = \frac{\gamma_p}{2\Gamma}\left(1 + \frac{1}{\beta}\right)\left(1 + \frac{1}{\zeta}\right) \tag{4}$$
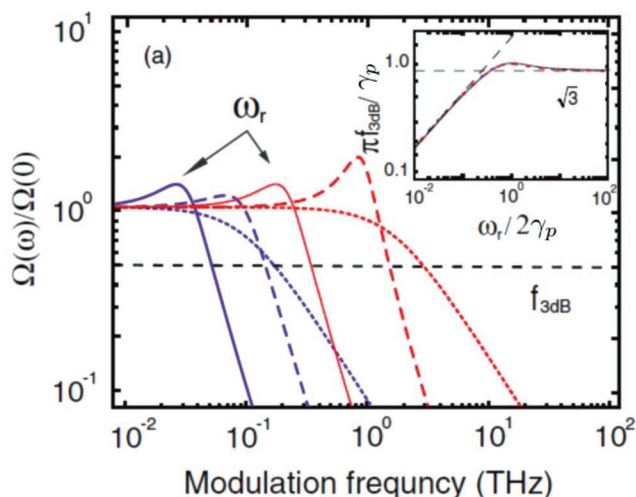
Figure 4. Calculated small signal modulation response for 1D (red curves) and 2D (blue curves) of plasmonic lasers using ideal four level emitters at 1.55 μm with pump rate R of $10R_{tr}$ (solid lines), $200R_{tr}$ (dashed lines), and ∞ (dotted line), respectively. Inset: the 3 dB modulation bandwidth. Reproduced with permission.[60] Copyright 2011, American Physical Society.

where $\zeta = \gamma_p/(\Gamma F_p \beta_0 A N_{tr})$, is the ratio of cavity loss γ_p to material loss $\Gamma F_p \beta_0 A N_{tr}$, which denotes the spontaneous emission rate in the transparent gain material.

Experimentally, the above-mentioned criterion can be implemented by measuring the second-order coherent degree $g^{(2)}(0)$ of the output using a Hanbury–Brown–Twiss (HBT) system,[78] and the lasing threshold is obtained when $g^{(2)}(0) \approx 1$.

2.4. Modulation Speed

It is worth to mention that, based on the rate equations neglecting nonradiative channels, Genov et al. theoretically investigated the possible modulation speed of a plasmonic nanolaser, and predicted a 3 dB bandwidth of small signal modulations.[60] As shown in **Figure 4**, the estimated modulation speed at visible (VIS) and near-infrared (NIR) region can go up to terahertz, benefited from the large Purcell factor and short cavity lifetime in a plasmonic nanolaser. The 3 dB modulation bandwidth follows a universal function (inset of Figure 4). At low pump rates, the bandwidth is limited by relaxation oscillations, $f_{3dB} = \sqrt{3}\omega_r/2\pi$,

where ω_r is the relaxation oscillation of the laser, saturating at $f_{3dB} = \sqrt{3}\gamma_p/2\pi$ for high pump rates due to cavity damping.

3. Material Issues

3.1. Plasmonic Materials

The choice of materials for the plasmonic cavity is critical for plasmonic lasing. **Figure 5** summarizes the complex dielectric constants $\varepsilon(\omega) = \varepsilon'(\omega) + i\varepsilon''(\omega)$ of 4 typical materials, silver (Ag), gold (Au), copper (Cu), and aluminum (Al) with wavelength ranging from 200 to 1200 nm. The real part of the dielectric constant (ε') describes the polarization response to the external electromagnetic field and the imaginary part (ε'') indicates the material loss.

From VIS to NIR, Ag has the smallest ε'' and thus the lowest loss. However, Ag is easily degraded in ambient environment via oxidation or sulfidation. A thin layer of insulator film (nanometer thickness) is helpful for alleviating the degradation, as has been used in the semiconductor–insulator–metal (SIM) configuration that will be discussed in Section 4.2.1. In contrast, Au is of very high chemical stability. Also, Au has the second smallest ε'', and has been most widely used for plasmonic waveguiding and localization. However, the intraband transition of Au presents a considerable loss with wavelength shorter than about 500 nm, limiting its use at a wavelength below 500 nm. Cu and Al are much less expensive materials than Ag and Au. Cu has a comparable ε'' to that of Au from about 600 nm to NIR, while Al possesses the lowest ε'' with wavelength shorter than 300 nm, and maintains a negative ε' with wavelength even below 200 nm. Besides, both Cu and Al are compatible with current nanoelectronics technologies, which is potential for the hybrid integration of nanoplasmonics with nanoelectronics system.

To further reduce the inherent loss, cooling is proved to be an effective method by reducing electron–electron and electron–phonon scattering and therefore increasing the mean free path of the SPP.[81] Another factor regarding the plasmonic loss is the structural quality of the material. Metal films grown by thermal evaporation or electron-beam evaporation usually present granular or polycrystalline structures with issues of surface roughness and grain boundaries, which may lead to additional damping of plasmonic propagation.[82] Recently, epitaxial Ag/Al films with atomically smooth surface have been grown on
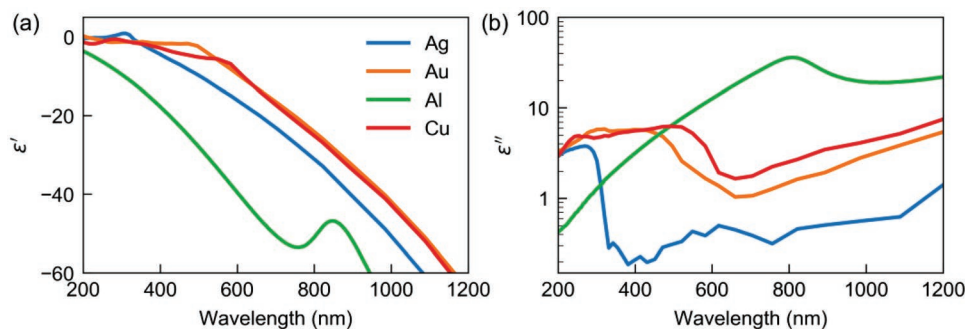

Figure 5. Optical properties of several metals for nanoplasmonics in the visible and near-infrared spectral regions. Both the real and imaginary parts of $\varepsilon(\omega) = \varepsilon'(\omega) + i\varepsilon''(\omega)$ are shown as functions of light wavelength in free space. Data were adapted from refs. [79,80].

some different dielectric platforms,[83,84] such as Ag on Si(111) and Al on Al$_2$O$_3$(0001). Owing to the ultralow surface roughness and excellent uniformity, these films exhibited the lowest loss reported ever. For example, the ε'' of a 45 nm epitaxial with 2 nm Al$_2$O$_3$/1.5 nm MgO capped Ag film is 2 times smaller at VIS region than that previously reported,[79,85] and from NIR to ultraviolet (UV), the ε'' of an epitaxial Al film on Al$_2$O$_3$ substrate is also smaller than previous data.[84,86]

The dispersion of SPP at lasing frequency, depending on the material and structural parameters, can also influence the lasing condition. Chou et al. and Sidiropoulos et al. reported that,[87,88] for a plasmonic nanolaser with semiconductor–insulator–metal configuration, when it was operated close to the surface plasmon frequency of the plasmonic material, it presented faster dynamics process, larger mode group index and smaller mode area.

In addition, besides the above-mentioned metals, some new plasmonic materials have been proposed.[89,90] Some transparent conduction oxides materials, e.g., indium tin oxide (ITO) and heavily doped zinc oxide (Al:ZnO and Ga:ZnO), exhibit metallic properties at NIR with smaller ε'' than Ag.[91] Also, some metal-nitrides like titanium nitride (TiN) and zirconium nitride (ZrN) exhibit metallic properties with comparable performances to Au in the VIS wavelengths.[92]

3.2. Gain Materials

To compensate the loss of a plasmonic cavity, active materials with high gain are desired in a plasmonic laser.

Inorganic semiconductors are commonly used solid gain materials in plasmonic nanolasers for their high gain, large refractive indices, feasibility of electric pump and wide gain range from UV to NIR. To conform the compactness of a plasmonic cavity, the gain materials are always fabricated into low-dimensional structures such as nanowires or nanopatches by nanofabrication approaches such as vapor–liquid–solid method or E-beam lithography. Binary II–VI semiconductors, such as ZnO, CdS, and CdSe can provide gain from UV to VIS and can be operated at room temperature due to their large exciton bonding energy.[93] III–V semiconductors with direct bandgaps such as GaN and GaAs are also excellent gain materials from UV to NIR. Especially, In$_x$Ga$_{1-x}$N is a kind of direct bandgap gain material with gain coefficient on the order of 10^3 mm^{-1} (up to 10^4 mm^{-1} in GaN) that is comparable with plasmonic loss of 200 dB mm^{-1} and can be tuned from NIR (InN, 0.65 eV) to UV (GaN, 3.4 eV).[94,95] An abundant classes of ternary and quaternary compound semiconductors (e.g., InGaAs and InGaAsP) have wide adjustable bandgaps, and can also be fabricated into versatile heterostructures and superlattices (e.g., quantum wells) to enhance the band-gap emission with enhanced density of states.[67] Another kind of heterostructures are core–shell In$_x$Ga$_{1-x}$N/GaN nanorods, which have been used to achieve ultralow-threshold plasmonic nanolasers.[95] Besides radial heterostructures, nanowires with axial heterostructures and quantum wells are also obtained.[96,97] Semiconductor quantum dots, which possesses quantum confinement in all three dimensions, can provide further enhancement in the density of states at the band edge to achieve higher gain with tunable spectral range.[23]

Organic dyes excel in their great varieties whose gain spectrum covering from near UV to NIR region, as well as broad gain spectral range. Meanwhile, dyes in solution can be readily adapted to all geometries, which simplify the design of the laser structures to some extent. However, under high-density excitation organic dyes are very likely to degrade due to photobleaching. Also, at high concentration, the quenching may occur. Perovskite is another type of promising gain materials, with generic chemical formula of AMX$_3$ or A$_2$MX$_4$, where A is an inorganic or organic cation (e.g., Cs$^+$ or CH$_3$NH$_3^+$, etc.), M is a divalent metallic cation (e.g., Pb$_2^+$, Sn$_2^+$, Mn$_2^+$, etc.), and X is halogen anion (I$^-$, Br$^-$, Cl$^-$).[98] Recently, perovskites have been attracting intensive attention due to their unprecedented success in photovoltaics and light-emitting devices.[99–101] As direct bandgap materials with high optical gain, flexible bandgap engineering, large absorption coefficient, and low defect state density, perovskites have been used as high gain materials in nanolasers.[98] For reference, optical gain of a MAPBI$_3$ perovskite thin film is reported to be around 320 mm^{-1}, which is as high as that of single-crystalline GaAs.[102] With bandgap engineering, the emission wavelength of perovskites can be tuned from UV to NIR.[98] Considering their favorable inherent material properties and possibilities to be synthesized as nanoplatelets, nanowires, and quantum dots, perovskite nanostructures are promising gain materials for plasmonic nanolasers.

4. Experimental Demonstrations of the Plasmonic Nanolasers

Experimentally, plasmonic nanolasers can be roughly categorized into three groups regarding the dimensions of optical confinement of the lasing cavity. As schematically depicted in **Figure 6**, in the 1D confinement case, the cavity mode propagating along a surface that presents tight confinement only at the direction perpendicular to the surface plane; in the 2D confinement, the cavity mode is confined along a 1D waveguide structure that exhibits tight confinement at the 2 dimensions perpendicular to the propagation direction; in the 3D confinement, the cavity mode is tightly localized in all three dimensions around the quasi 0D structure. Generally, with confinement well beyond the diffraction limit, the difficulties in realizing a plasmonic nanolaser increases with increasing dimensions of confinement, as a trade-off of the optical confinement and loss.
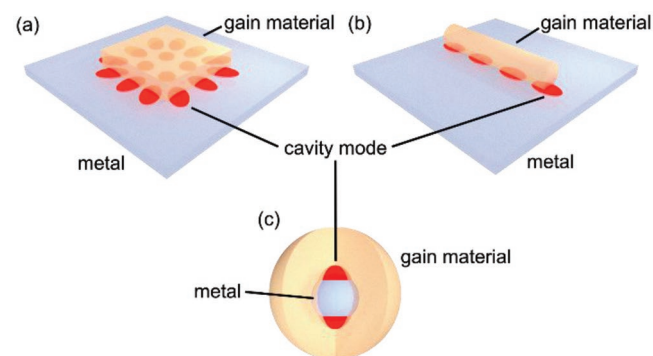

Figure 6. Schematic configurations of typical plasmonic nanolasers with lasing mode of a) 1D, b) 2D, and c) 3D confinement, respectively.

ADVANCED
SCIENCE NEWS
www.advancedsciencenews.com

ADVANCED
OPTICAL
MATERIALS
www.advopticalmat.de

In this section, we review up-to-date experimental endeavors to realize plasmonic nanolasers with increasing dimensions of confinement of the cavity mode, i.e., from 1D, 2D to 3D confinement. To be more focus, we introduce only typical configurations with cavity mode tightly confined at least on one dimension, and apologize for the incompleteness in our enumeration. In addition, several other types of plasmonic lasers with nanoscale feature sizes are also briefly mentioned.

4.1. 1D Confinement

4.1.1. Metal–Insulator–Metal Configuration

A metal–insulator–metal (MIM) structure can efficiently confine light between its two metal walls below the diffraction limit. In 2009, Hill et al. first demonstrated a plasmonic laser based on MIM configuration where III–V (InGaAs) gain materials were confined by two Ag walls and thin SiN insulator layers were used to separate them to reduce quenching as shown in **Figure 7**a.[34] The thickness of the semiconductor layer can be as small as 90 nm, which is well below the diffraction limit, and can support a highly confined TM_{01} mode. Vertical confinement is achieved by the index difference between the InGaAs and InP. The reflection at the end of the waveguide formed a Fabry–Perot (F–P) cavity. Due to the long cavity length (several micrometers), a cavity Q-factor of 370 was obtained at cryogenic temperature. The nanolaser emitted light at telecommunication wavelength by electric injection as shown in Figure 7b. While thin MIM configuration required cryogenic temperatures for lasing, a wider (310 nm) semiconductor cores, which could support a photonic mode, allowed for room-temperature operation. Later, a plasmonic laser with similar structure but using distributed feedback was demonstrated with a semiconductor core of about 140 nm,[103] which can be operated at room temperature with a relatively high Q-factor (≈300).

4.1.2. 1D Confined Semiconductor–Insulator–Metal Configuration

Another widely used 1D configuration is a semiconductor nanopatch on a metal substrate separated by a thin low-index insulator layer, which supports a low-loss hybrid mode with field strongly confined in the low-index insulator layer.[105] Considered as coupling between the plasmonic and waveguide modes across the gap, this hybrid mode enables "capacitor-like" energy storage that can achieve great balance between mode confinement and propagating loss, which can also be tuned easily by changing the refractive index or thickness of the insulator gap. In addition, the insulator gap is also helpful for reducing the quenching caused by the excitation of lossy surface wave and electron-hole pairs in the metal.[69–71] In 2011, Ma et al. reported a room-temperature plasmonic nanolaser around 500 nm using a CdS nanosquare with thickness of 45 nm and width of 1 μm, as illustrated in Figure 7c.[57] The hybrid SPP mode with a $\lambda/20$ confinement was reflected on the side boundary of the CdS nanosquare, resulting in a Purcell factor of 18 and a quality factor approaching 100. By controlling the structural geometry, single-mode lasing was also demonstrated (Figure 7d).

Further improvements on this kind of laser configuration for high stability[106] or high external quantum efficiency[107] were also demonstrated. Compared with conventional broadband plasmonic resonance, the lasing action significantly narrows the resonance band and enhances the output signal, making it potential for high-sensitivity plasmonic sensing.[108–110]

4.1.3. Single-Interface SPP F–P Cavity

Recently, Kress and Cui et al. reported plasmonic lasers based on single-interface SPP mode at room temperature.[104] As shown in Figure 7e, the cavity SPP mode on the Ag/air interface was reflected by two Ag block reflectors to form a concave F–P cavity. The total cavity length is 10 μm, and colloidal quantum dots were deposited along the cavity to serve as gain materials. The high quality factor in this design leads to a linewidth down to 0.65 nm (Figure 7f). With similar configuration, Zhu et al. achieved room-temperature lasing by leveraging surface plasmons propagating in an open Fabry–Perot cavity formed by a flat metal surface coated with a subwavelength-thick layer of optically pumped gain medium that was orthogonally bound by a pair of flat metal sidewalls.[111] For efficient extraction of energy from the F–P cavity, specific designs were introduced in both works such as an elongated reflector or grooves.

4.2. 2D Confinement

4.2.1. Transversely Hybridized Lasing Cavity

A plasmonic nanolaser cavity with 2D confinement usually relies on 1D waveguide structures such as nanowires. In 2009, Oulton et al. reported a 2D-confined plasmonic nanolaser using a low-loss hybrid plasmonic mode generated by placing a CdS semiconductor nanowire on the top of a Ag substrate, separated by a nanometer-thickness MgF_2 layer[35] as shown in **Figure 8**a. The CdS nanowire is also used as the gain material under optical excitation. The estimated cross-sectional mode area of the hybrid plasmonic-photonic mode could be down to $\lambda^2/400$. Lasing output was observed around 489 nm wavelength at a temperature below 10 K (Figure 8b). Compared with photonic lasing in a CdS nanowire on a MgF_2 substrate that shows cut off when the nanowire diameter is smaller than about 140 nm, the hybrid plasmonic lasing mode maintains with diameter down to 52 nm. When the thickness of the MgF_2 layer decreases to 5 nm, a Purcell factor of ≈6 and a maximum β of ≈0.8 was obtained. Meanwhile, the tight confinement leads to high loss of the lasing cavity, which consequently leads to a high lasing threshold (≈60 MW cm^{-2} in pumping density).

In order to reduce the lasing threshold, broaden the lasing spectrum, operate the laser at room temperature, or pursue even tighter optical confinement of the lasing mode, a number of successful efforts have been reported with similar 2D-confined configuration afterward.

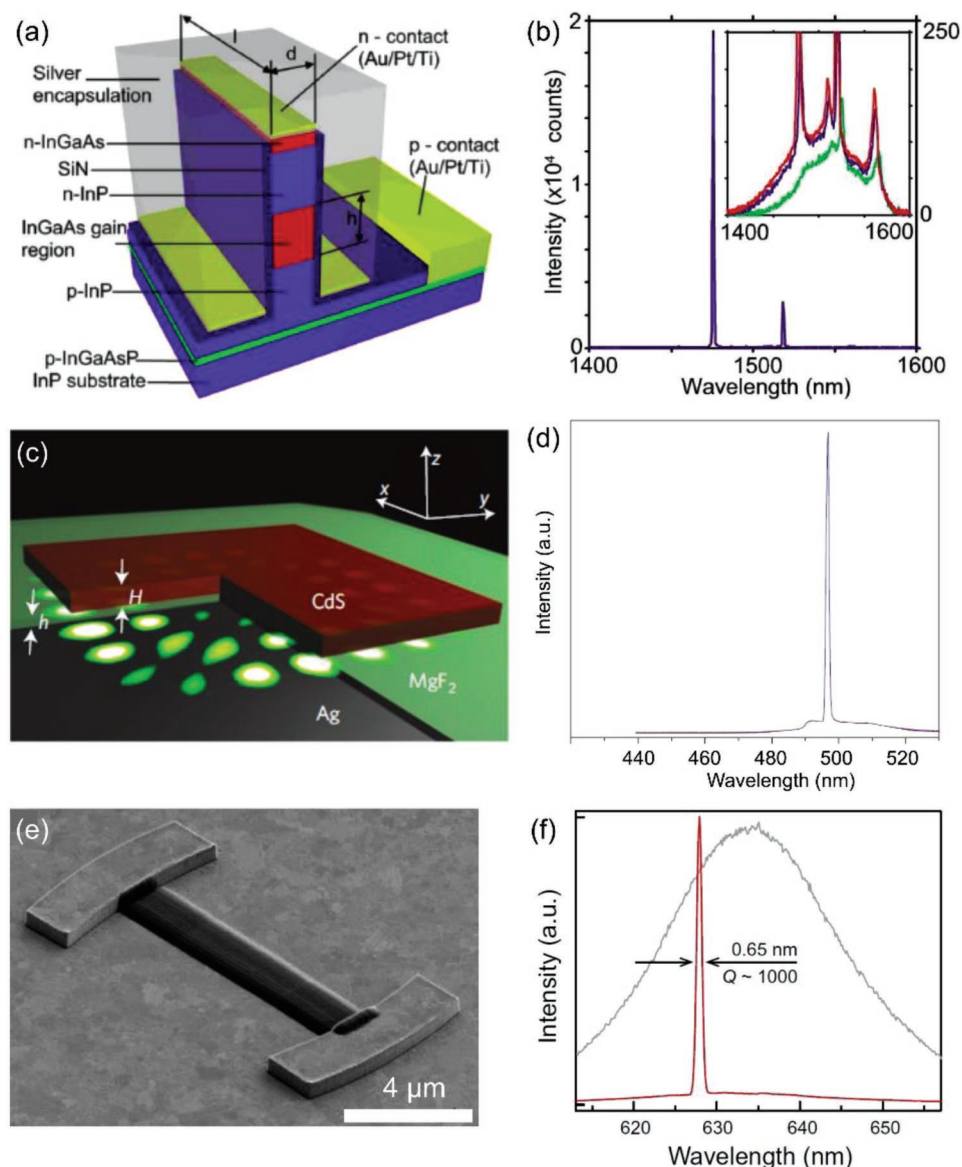Benefited from the diverse semiconductor materials, the lasing spectrum has been extended to UV[84,87,88,112–119] and

ADVANCED
SCIENCE NEWS
www.advancedsciencenews.com

ADVANCED
OPTICAL
MATERIALS
www.advopticalmat.de

Figure 7. 1D-confined plasmonic nanolasers. a) Structure of cavity formed by a rectangular semiconductor pillar encapsulated in Ag and b) above threshold emission spectrum with pump current of 180 µA at 78 K.[34] Inset: emission spectra for 20 (green), 40 (blue), and 60 (red) µA at 78 K, respectively. c) Schematic diagram of a plasmonic laser composed of a thin CdS square atop a Ag substrate separated by a 5 nm MgF$_2$ gap, with d) lasing emission spectrum at a pumping density of 3074 MW cm^{-2}.[57] e) SEM image of a plasmonic cavity with two ≈600 nm tall Ag block reflectors positioned 10 µm apart on an ultrasmooth Ag surface. Colloidal quantum dots are deposited a stripe (≈100 nm thick and ≈2 mm wide) between the reflectors. f) Emission spectrum above threshold (red) and broad photoluminescence spectrum from quantum dots on flat Ag (outside the cavity) (gray).[104] a,b) Reproduced with permission.[34] Copyright 2009, Optical Society of America. c,d) Reproduced with permission.[57] Copyright 2011, Nature Publishing Group. e,f) Reproduced with permission.[104] Copyright 2017, American Association for the Advancement of Science.

NIR[120–125] that covering the whole VIS region.[83,95–97,126–129] For example, in 2014, Lu et al. demonstrated an all-color plasmonic nanolasers with ultralow thresholds using In$_x$Ga$_{1−x}$N/GaN core–shell nanorods supported on an Al$_2$O$_3$-capped epitaxial Ag film (Figure 8c).[95] Broadband tunable, single-mode plasmonic lasing was observed in the full visible spectrum (468–642 nm) with working temperature up to 120 K (Figure 8d).

Meanwhile, instead of natural reflection occurred at the end-facet of the nanowire, the feedback in SIM configuration have also

been demonstrated by using plasmonic Bragg structures,[130,131] total internal reflection,[57,126,127] and ring cavity.[124,127]

To reduce the lasing threshold, a number of efforts, including improving surface quality of the plasmonic materials[82,84,116,117] and using higher gain materials[83,95,112] have been successfully made. Especially, based on the axial InGaN/GaN quantum wells and Ag substrate (Figure 8e,f), Tao et al. realized a room-temperature continuous-wave-pumped plasmonic nanolaser at 490 nm wavelength with threshold down to 300 W cm^{-2}.[97]

**ADVANCED
SCIENCE NEWS**

www.advancedsciencenews.com

**ADVANCED
OPTICAL
MATERIALS**
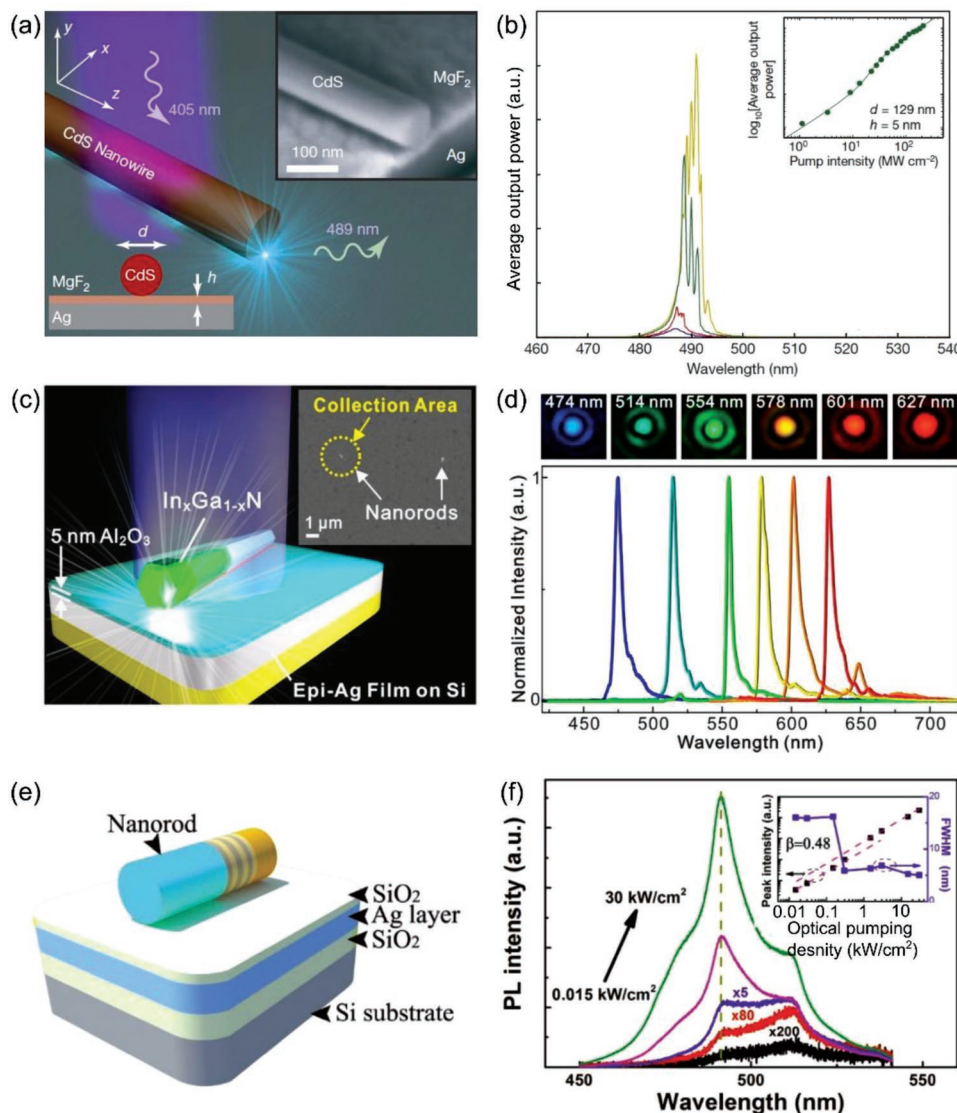
www.advopticalmat.de

Figure 8. 2D-confined plasmonic nanolasers with transversely hybridized cavity modes. a) Schematic diagrams of a plasmonic laser consisted of a CdS nanowire on the top of a Ag substrate, separated by a nanometer thickness MgF$_2$ layer. Inset: SEM image of the device. b) Emission spectrum at pump densities of 21.25 MW cm^{-2} (purple), 32.50 MW cm^{-2} (red), 76.25 MW cm^{-2} (green), and 131.25 MW cm^{-2} (yellow), respectively.[35] Inset: log scale pump-output curve. c) Schematic diagram of a plasmonic laser with a single In$_x$Ga$_{1-x}$N@GaN core–shell nanorod placed on an Al$_2$O$_3$-covered epitaxial Ag film. Inset: SEM image of the device. d) All-color, single-mode lasing images and corresponding emission spectrum observed from single nanorods.[95] e) Schematic diagram of a InGaN/GaN elliptical nanorod supported on a SiO$_2$-capped Ag film, with f) emission spectrum at varying pump densities.[97] Inset: log-scale pump-output curve and linewidth evolution. a,b) Reproduced with permission.[35] Copyright 2009, Nature Publishing Group. c,d) Reproduced with permission.[95] Copyright 2014, American Chemical Society. e,f) Reproduced with permission.[97] Copyright 2017, Wiley-VCH.

To pursue tighter optical confinement, in 2014, based on a laser structure consisted of triangular GaN nanowire on the top of a SiO$_2$ coated Al substrate, Zhang et al. reported room-temperature lasing at the wavelength of 375 nm,[112] with a mode area of 0.0147λ^2. In 2017, Chou et al. concentrated the transverse mode area down to 0.0013λ^2 using a 35 nm side hexagonal ZnO nanowire on a Ag substrate coated with a 7 nm thickness SiO$_2$ gap. When the laser system was operated at 77 K, lasing at 371 nm was observed.[88]

In addition, it is worth to note that, to reduce the metal loss, a nanoscale insulator gap is essential for reducing lasing threshold of hybrid plasmonic modes in above-mentioned structures. Such a gap can also be provided by the insulator shell of a nanowire, the first layer of quantum wells or a high-order hybrid mode with lower loss.[120,122,124] For reference, in 2016, Chou et al. investigated a hybrid laser structure of a ZnO nanowire on a single-crystalline Al substrate.[115] Without an insulator layer, the average lasing threshold was about 20 MW cm^{-2}, while that increased to 80 MW cm^{-2} with additional insulator layer. The divergent threshold value due to the introduction of additional insulator layer was attributed to the fluctuating surface quality after the deposition of the insulator layer.
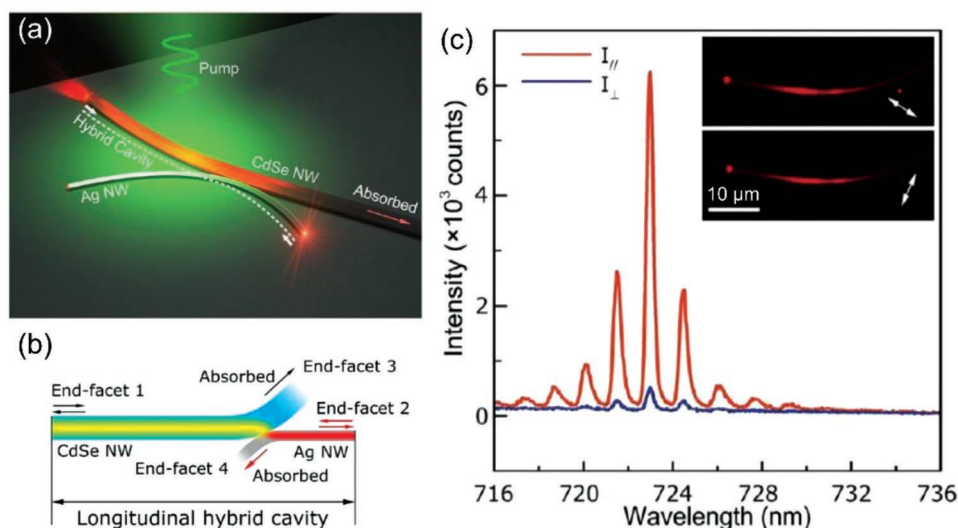
ADVANCED
SCIENCE NEWS
www.advancedsciencenews.com

ADVANCED
OPTICAL
MATERIALS
www.advopticalmat.de

Figure 9. Longitudinally hybridized photon–plasmon NW laser. a,b) Schematic illustration of the hybrid photon–plasmon NW laser, which is composed of a Ag NW and a CdSe NW coupled into X-shape. The right segment of CdSe NW serves as a distributed absorber without reflection. The coupled hybrid cavity (marked by the dashed line) serves as the hybrid photon–plasmon lasing cavity. c) Polarization-sensitive lasing spectra from Ag NW end-facet, with the emission polarization oriented parallel (red line) and perpendicular (blue line) to the Ag NW. Inset, dark-field microscope images show the polarization-dependent lasing outputs. Scale bar: 10 μm. The white arrows indicate the directions of the polarization. Reproduced with permission.[132] Copyright 2013, American Chemical Society.

4.2.2. Longitudinally Hybridized Lasing Cavity

Besides the transversely coupled metal–dielectric structures that support hybrid SPP modes with polarization perpendicular to the propagation direction, the hybrid photon–plasmon cavity can also be realized by a longitudinal coupling scheme. In 2013, Wu et al. reported a plasmonic lasing structure based on a longitudinally hybridized cavity.[132] As shown in **Figure 9**a, the hybrid lasing cavity is formed by coupling a 100 nm diameter Ag nanowire to a CdSe nanowire with a measured photon–plasmon coupling efficiency of 20%. Using end-facet reflection from each nanowire as feedback, the lasing mode circulating inside the cavity was alternatively changed between photonic mode in the CdSe nanowire and plasmonic mode in the Ag nanowire, and offered a far-field spatially separable plasmonic lasing mode on the Ag nanowire (Figure 9b). By optically pumping the CdSe nanowire at room temperature, lasing emission from the plasmonic mode supported by the Ag nanowire was observed (Figure 9c) around 723 nm wavelength, with an estimated mode area of $0.008\lambda^2$.

4.3. 3D Confinement

To pursue the extreme confinement of optical fields in 3D, localized surface plasmon oscillation has been investigated in metal nanoparticles with particle sizes down to several nanometers, which is expected to be only limited by nonlocal effect (≈1 nm).[133] Generally, with increasing confinement, optical loss of the localized surface plasmon resonance (LSPR) modes increases, and the interfacing efficiency between the LSPR and free-space fields decreases drastically. However, there is a possibility to use a single metal nanoparticle or other quasi 0D structures as a lasing nanocavity with 3D confinement, if the

confinement is compromised to a certain extent. Since the first theoretical model of plasmonic nanolaser,[33] great efforts have been made to pursue the 3D-confined LSPR nanolaser.[49,134–137] Although lasing emission from active nanostructure ensemble composing of an Au nanosphere core and a layer of dye molecules shell was observed,[134] but lasing from a single nanoparticle had not been confirmed, and the lasing cavity is more likely originated from other mechanisms (e.g., random lasing) than the single-particle LSPR feedback. Although a number of follow-up works of similar configurations were reported for biophotonic applications,[138,139] realizing a lasing nanoplasmonic cavity with 3D tight confinement remains challenging. In that case, the further efforts in realizing plasmonic lasing in single 3D-confined cavity may bring new opportunities for biophotonics on a smaller scale (e.g., molecular scale).

A complementary cavity configuration is a bowtie structure, which is composed of metal nanoparticle dimers with a nanometer-size gap to localize and enhance of electric fields with LSPR. In 2012, Suh et al. reported a plasmonic bowtie nanolasers array with organic dye molecules as gain materials at room temperature.[59] As shown in **Figure 10**a,b, the bowtie structure with a 35 nm gap supported a bonding gap mode with mode volume down to $0.0004(\lambda/2n)^3$ and quality factor of ≈35, corresponding to a Purcell factor of ≈300. The period of the array, i.e., the distance between two neighboring bowtie structures, is 1200 nm, which is large enough to suppress the coupling between neighboring bowtie structures that may otherwise lead to surface lattice plasmonic mode. Pumped by 800 nm wavelength femtosecond pulses (45 fs pulsewidth, 1 kHz repetition), lasing emission at 800 nm wavelength was observed from the bowtie array (Figure 10f). However, lasing emission from a single bowtie structure was not confirmed experimentally.

Very recently, Kewes et al. demonstrated a semiclassical analytic model for spherical core–shell nanoparticle plasmonic
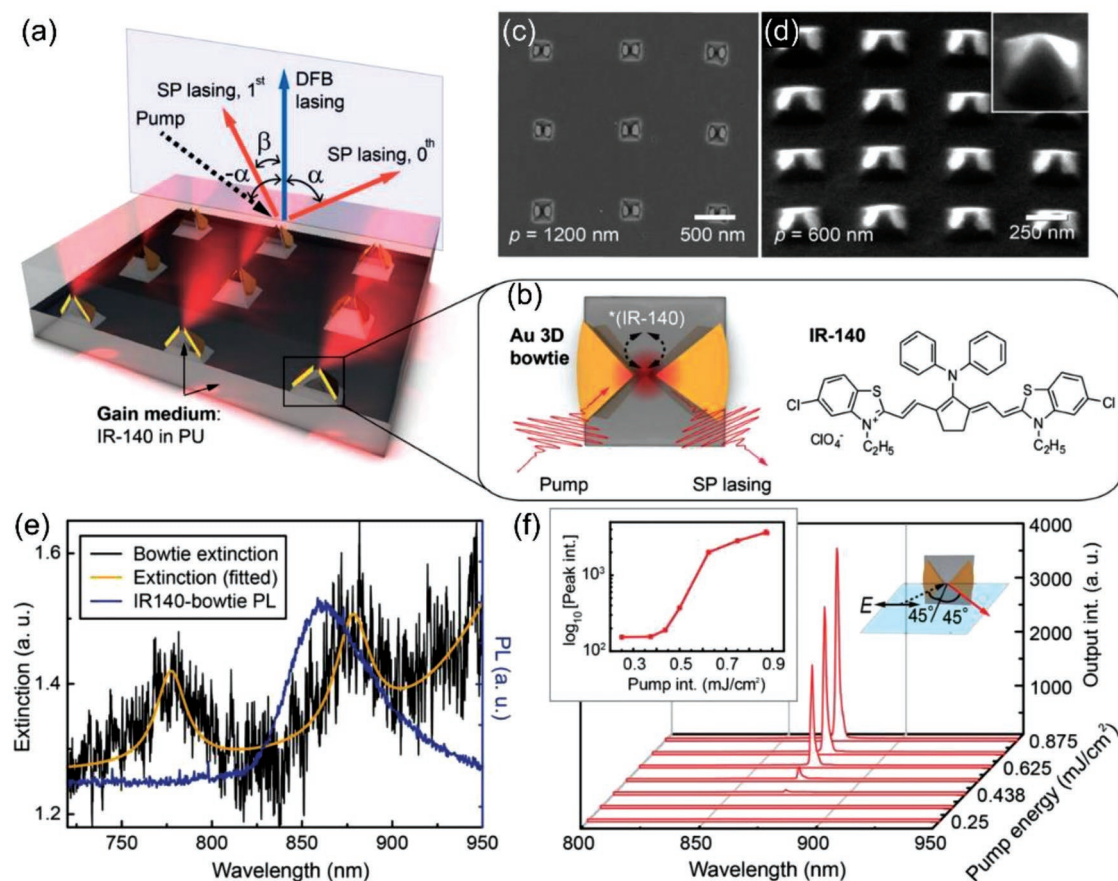
1900334 (10 of 16)

**ADVANCED
SCIENCE NEWS**
www.advancedsciencenews.com

**ADVANCED
OPTICAL
MATERIALS**
www.advopticalmat.de

Figure 10. 3D-confined plasmonic nanolasers. a) Scheme of array and b) an individual unit of 3D bowtie plasmonic lasers using IR-140 dye molecules as gain materials, with SEM images of bowtie array with period of c) 1200 nm and d) 600 nm, respectively. e) Photoluminescence spectrum of IR-140 and extinction spectrum of Au bowties with period of 1200 nm, with f) emission spectrum under pump polarization parallel to the dimer axis.[59] Inset: pump–output curve. Reproduced with permission.[59] Copyright 2012, American Chemical Society.

lasers.[68] They used a fully electromagnetic Mie theory to incorporate high-order-mode enhanced nonradiative channels, and showed that the near-field coupling between emitters and the plasmonic nanosphere does not only strengthen the Purcell effect of emitting to dipole mode but also higher order modes, which undermine and even reverse the beneficial effects of the strong Purcell effect in such system, resulting in an extremely or unreachably high gain required for realizing single-nanoparticle lasing.

4.4. Other Configurations

Besides the above-mentioned systems, many other configurations for plasmonic lasers have been demonstrated using cavity modes from surface lattice plasmon mode in metal nanoparticles array,[66,140–162] Tamm SPP mode,[163–165] long-range SPP mode,[166–168] random mode[169–174] to other diverse modes.[175–189] Also, by operating at NIR region with relatively low metal losses, metal-cladded 3D-confined subdiffraction-limit plasmonic nanolasers have been demonstrated,[58,190–194] in which the cladding metals support TM cavity modes and behave more like perfect reflecting mirrors.[38] In addition, a new category of plasmon-assisted nanolasers are also demonstrated

recently, using plasmonic effect to enhance the pumping intensity or reduce the output mode size.[195–202] However, the confinement of the lasing modes in these systems are usually compromised, and we will not go into details here.

5. Discussion and Conclusion

So far we have briefly reviewed the recent works in developing plasmonic nanolasers with cavity size below the diffraction limit at least in one dimension. As nanolasers with smaller cavity mode or "beam" size is always desired with increasing demands in nanoscale optical sensing, metrology, imaging, storage, and on-chip circuitry,[30,31,203,204] the plasmonic nanolaser provides a unique approach toward these applications. However, to shrink the lasing cavity far below the diffraction limit, challenges increase with decreasing mode size as discussed below.

First of all, we summarize the mode-volume-dependent lasing threshold (in terms of pumping density) of typical plasmonic lasers demonstrated experimentally in a plot shown in **Figure 11**. For better clarity, we consider three typical operation temperature regions of 300 K (room temperature), ≈80 K (liquid nitrogen) and <10 K (liquid helium), and include those with cavity volume V/λ^3

**ADVANCED
SCIENCE NEWS**

www.advancedsciencenews.com

**ADVANCED
OPTICAL
MATERIALS**
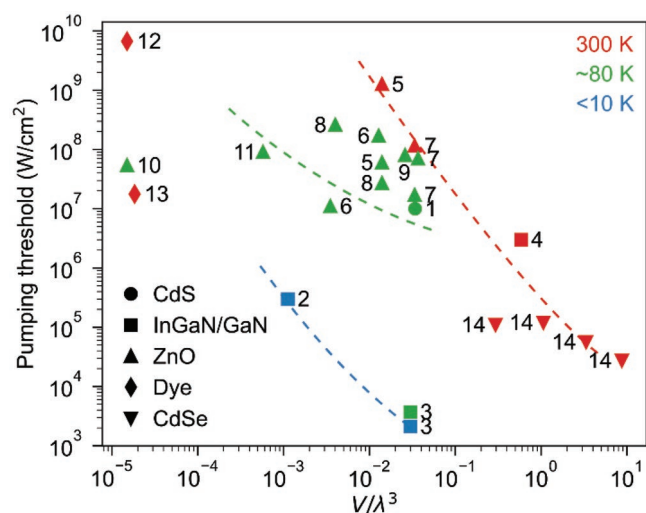
www.advopticalmat.de

Figure 11. Pumping thresholds and effective mode volume of some plasmonic nanolasers with gain materials of CdS (circle), InGaN/GaN (square), ZnO (triangle up), dyes (diamond), and CdSe (triangle down) under temperatures of <10 K (blue), ≈80 K (green), and 300 K (red), respectively. Data were adapted from following references. 1: ref. [35]; 2: ref. [126]; 3: ref. [83]; 4: ref. [112]; 5: ref. [113]; 6: ref. [114]; 7: ref. [115]; 8: ref. [88]; 9: ref. [117]; 10: ref. [187]; 11: ref. [131]; 12: ref. [59]; 13: ref. [134]; 14: ref. [205].

down to 10^{-5} level, while similar dependence in larger plasmonic cavities ($V/\lambda^3 > 0.1$) has been nicely demonstrated recently.[205]

It is obvious that, despite of the different plasmonic (e.g., Au, Ag, or Al) and gain (e.g., Dye, ZnO, InGaN/GaN, CdS, and CdSe) materials, at the same temperature, the lasing threshold increases with decreasing mode volume. Meanwhile, with similar mode volume, the lasing threshold decreases with decreasing temperature, in accordance with lower plasmonic loss at lower temperature.[81] The large deviation of the lasing threshold (e.g., of point #13) may indicate that the lasing mode is not localized by the single-particle surface plasmon resonance (SPR).

Second, as the most important and unique advantage of a plasmonic nanolaser, a mode size far below the diffraction limit, e.g., $\lambda/20$ in at least one dimension, has been experimentally demonstrated. However, extending this confinement to three dimensions (i.e., $V/\lambda^3 \approx 10^{-4}$) is rather difficult due to the significantly increasing loss. General solutions are searching better gain and plasmonic materials, as well as higher efficiency cavity design for supporting lower loss cavity modes and surviving higher pumping intensity, and this should work to some extent. However, at optical frequency from UV to NIR, the commonly used metals, Al (UV), Ag (from VIS to NIR), and Au (NIR) are among the best materials regarding the plasmonic loss,[89] and there is also not much space to reduce the loss via geometric design when the SPR mode volume is far below the diffraction limit.[206] Noticeably, using photon–plasmon hybrid modes is an excellent route to low-loss cavity mode,[105] but the effective area of this kind of hybrid mode is difficult to be scaled down when it reaches a certain value (typically >$\lambda/50$), where the amount of induced charge within the effective volume of the dielectric is not large and efficient enough to support the plasmonic oscillation at the optical frequency.

Another possible route is decreasing the operation temperature to reduce the plasmonic loss in metal, and/or increase the quantum efficiency of the gain material. As shown in Figure 11, using the same gain material of ZnO and plasmonic material of Ag, the threshold of point #5 at 77 K (60 MW cm^{-2}) is much lower than that of at 300 K (1262 MW cm^{-2}), showing the potential to achieve smaller lasing cavity at lower temperature.

Meanwhile, the reduction of mode size will enhance Purcell effect and thus the spontaneous emission rate, which is otherwise advantageous for enhancing stimulated emission rate, may deplete the excited carriers in a plasmonic nanolaser with a large Purcell factor, resulting in obvious increase in lasing threshold or failure to reach inversion population.[87]

On the other hand, if we compromise the tight confinement from 3D to 2D/1D, there seem possibilities of significantly reducing the mode size. For example, while the calculated threshold of an electric-injection 3D-confined plasmonic nanolaser is insufferably high (e.g., ≈MA cm$^{-2[54]}$), that for a 1D-confined SIM plasmonic nanolaser increases moderately when the cavity size was decreased below the diffraction limit.[205] Also, appropriate design of the cavity structure, e.g., coupling waveguide-type plasmonic and gain structures into a longitudinally hybridized plasmon–photon cavity,[132] can offer much higher gain than transversely coupled system, and is thus possible to compensate the loss of a cavity mode with much tighter confinement. Furthermore, in some 2D materials (e.g., single-layer graphene), it is possible to excite plasmonic mode with confinement down to ≈$\lambda/50$ in at least one dimension within MIR spectral range,[207–211] which might be shifted to NIR by mean of doping effects.[209,212]

Recently, identification and reduction of the lasing threshold in a plasmonic nanolaser has been attracting increasing attentions. The turning point on the input–output plot, which is typically used to identify the threshold of a conventional laser, becomes vague in a nanolaser with decreasing cavity size due to the significantly enhanced spontaneous emission and nonradiation processes. As shown in Equation (4), to reduce the lasing threshold, low cavity loss, high β and large ζ, or small material loss, are in demand. The low cavity loss in a small cavity will lead to large Purcell effect, which will enhance both spontaneous and stimulated emission rate and is possible to achieve large β (i.e., $\beta \approx 1$). However, the enhanced spontaneous, as well as the enhanced nonradiative channels via high-order modes of the plasmonic cavity, will also deplete the excited carriers, resulting in confinement-induced gain reduction and material loss. Meanwhile, with $\beta \approx 1$, the turning point on the input-output plot is smeared and the lasing oscillation looks like "threshold-less." Experimentally, from the first-order coherence, linewidth and directionality that are largely determined by the cavity, it is difficult to distinguish the spontaneous emission from the stimulated emission, measuring the second-order coherence with an HBT setup will be a feasible approach, which may also serve as a much stricter criterion for the lasing threshold.

Finally, despite of the great challenges in pursuing the extreme lasing conditions in plasmonic nanolasers, abounding phenomena or effects of light–matter interaction, previously neglectable in conventional lasers, become prominent in nanolasers, which has greatly extend the principle and technical boundaries of a lasing system. Also, from the material aspect,

**ADVANCED
SCIENCE NEWS**

www.advancedsciencenews.com

**ADVANCED
OPTICAL
MATERIALS**

www.advopticalmat.de

non-classical materials or structures, e.g., strongly correlated system for plasmonic response with tighter confinement[213] or Bose–Einstein condensed system with lower lasing threshold,[66,214] may be introduced to surpass the current challenges regarding the confinement and the loss, if the compromise in other aspects is acceptable.

Conflict of Interest

The authors declare no conflict of interest.

Keywords

[1] A. E. Siegman, *Lasers*, University Science Books, Mill Valley, CA, USA **1986**.

[2] T. H. Maiman, *Nature* **1960**, *187*, 493.

[3] M. J. Edwards, P. K. Patel, J. D. Lindl, L. J. Atherton, S. H. Glenzer, S. W. Haan, J. D. Kilkenny, O. L. Landen, E. I. Moses, A. Nikroo, R. Petrasso, T. C. Sangster, P. T. Springer, S. Batha, R. Benedetti, L. Bernstein, R. Betti, D. L. Bleuel, T. R. Boehly, D. K. Bradley, J. A. Caggiano, D. A. Callahan, P. M. Celliers, C. J. Cerjan, K. C. Chen, D. S. Clark, G. W. Collins, E. L. Dewald, L. Divol, S. Dixit, T. Doeppner, D. H. Edgell, J. E. Fair, M. Farrell, R. J. Fortner, J. Frenje, M. G. G. Johnson, E. Giraldez, V. Y. Glebov, G. Grim, B. A. Hammel, A. V. Hamza, D. R. Harding, S. P. Hatchett, N. Hein, H. W. Herrmann, D. Hicks, D. E. Hinkel, M. Hoppe, W. W. Hsing, N. Izumi, B. Jacoby, O. S. Jones, D. Kalantar, R. Kauffman, J. L. Kline, J. P. Knauer, J. A. Koch, B. J. Kozioziemski, G. Kyrala, K. N. LaFortune, S. Le Pape, R. J. Leeper, R. Lerche, T. Ma, B. J. MacGowan, A. J. MacKinnon, A. Macphee, E. R. Mapoles, M. M. Marinak, M. Mauldin, P. W. McKenty, M. Meezan, P. A. Michel, J. Milovich, J. D. Moody, M. Moran, D. H. Munro, C. L. Olson, K. Opachich, A. E. Pak, T. Parham, H.-S. Park, J. E. Ralph, S. P. Regan, B. Remington, H. Rinderknecht, H. F. Robey, M. Rosen, S. Ross, J. D. Salmonson, J. Sater, D. H. Schneider, F. H. Seguin, S. M. Sepke, D. A. Shaughnessy, V. A. Smalyuk, B. K. Spears, C. Stoeckl, W. Stoeffl, L. Suter, C. A. Thomas, R. Tommasini, R. P. Town, S. V. Weber, P. J. Wegner, K. Widmann, M. Wilke, D. C. Wilson, C. B. Yeamans, A. Zylstra, *Phys. Plasmas* **2013**, *20*, 070501.

[4] P. B. Corkum, F. Krausz, *Nat. Phys.* **2007**, *3*, 381.

[5] J. Klein, J. D. Kafka, *Nat. Photonics* **2010**, *4*, 289.

[6] M. F. Ciappina, J. A. Perez-Hernandez, A. S. Landsman, W. A. Okell, S. Zherebtsov, B. Foerg, J. Schoetz, L. Seiffert,

[7] T. Fennel, T. Shaaran, T. Zimmermann, A. Chacon, R. Guichard, A. Zaier, J. W. G. Tisch, J. P. Marangos, T. Witting, A. Braun, S. A. Maier, L. Roso, M. Krueger, P. Hommelhoff, M. F. Kling, F. Krausz, M. Lewenstein, *Rep. Prog. Phys.* **2017**, *80*, 054401.

[7] M. T. Hassan, *J. Phys. B: At., Mol. Opt. Phys.* **2018**, *51*, 032005.

[8] E. Murphy, *Nat. Photonics* **2010**, *4*, 287.

[9] G. Roelkens, L. Liu, D. Liang, R. Jones, A. Fang, B. Koch, J. Bowers, *Laser Photonics Rev.* **2010**, *4*, 751.

[10] Z. Zhou, B. Yin, J. Michel, *Light: Sci. Appl.* **2015**, *4*, e358.

[11] R. N. Hall, G. E. Fenner, J. D. Kingsley, T. J. Soltys, R. O. Carlson, *Phys. Rev. Lett.* **1962**, *9*, 366.

[12] M. I. Nathan, W. P. Dumke, G. Burns, F. H. Dill, G. Lasher, *Appl. Phys. Lett.* **1962**, *1*, 62.

[13] Z. I. Alferov, *Rev. Mod. Phys.* **2001**, *73*, 767.

[14] J. Vanderziel, R. Dingle, R. Miller, W. Wiegmann, W. Nordland, *Appl. Phys. Lett.* **1975**, *26*, 463.

[15] H. Soda, K.-i. Iga, C. Kitahara, Y. Suematsu, *Jpn. J. Appl. Phys.* **1979**, *18*, 2329.

[16] K. Iga, *IEEE J. Sel. Top. Quantum Electron.* **2000**, *6*, 1201.

[17] S. L. McCall, A. F. J. Levi, R. E. Slusher, S. J. Pearton, R. A. Logan, *Appl. Phys. Lett.* **1992**, *60*, 289.

[18] R. E. Slusher, A. F. J. Levi, U. Mohideen, S. L. McCall, S. J. Pearton, R. A. Logan, *Appl. Phys. Lett.* **1993**, *63*, 1310.

[19] Y. Zhang, C. Hamsen, J. T. Choy, Y. Huang, J.-H. Ryou, R. D. Dupuis, M. Loncar, *Opt. Lett.* **2011**, *36*, 2704.

[20] O. Painter, R. K. Lee, A. Scherer, A. Yariv, J. D. O'Brien, P. D. Dapkus, I. Kim, *Science* **1999**, *284*, 1819.

[21] Y. Akahane, T. Asano, B.-S. Song, S. Noda, *Nature* **2003**, *425*, 944.

[22] P. Lalanne, C. Sauvan, J. P. Hugonin, *Laser Photonics Rev.* **2008**, *2*, 514.

[23] V. I. Klimov, *Science* **2000**, *290*, 314.

[24] P. Bhattacharya, S. Ghosh, A. D. Stiff-Roberts, *Annu. Rev. Mater. Res.* **2004**, *34*, 1.

[25] M. H. Huang, S. Mao, H. Feick, H. Q. Yan, Y. Y. Wu, H. Kind, E. Weber, R. Russo, P. D. Yang, *Science* **2001**, *292*, 1897.

[26] Y. Xiao, C. Meng, P. Wang, Y. Ye, H. K. Yu, S. S. Wang, F. X. Gu, L. Dai, L. M. Tong, *Nano Lett.* **2011**, *11*, 1122.

[27] S. W. Eaton, A. Fu, A. B. Wong, C.-Z. Ning, P. Yang, *Nat. Rev. Mater.* **2016**, *1*, 16028.

[28] M. T. Hill, M. C. Gather, *Nat. Photonics* **2014**, *8*, 908.

[29] M. Nomura, N. Kumagai, S. Iwamoto, Y. Ota, Y. Arakawa, *Opt. Express* **2009**, *17*, 15975.

[30] D. K. Gramotnev, S. I. Bozhevolnyi, *Nat. Photonics* **2010**, *4*, 83.

[31] M. L. Brongersma, V. M. Shalaev, *Science* **2010**, *328*, 440.

[32] X. Guo, Y. B. Ying, L. M. Tong, *Acc. Chem. Res.* **2014**, *47*, 656.

[33] D. J. Bergman, M. I. Stockman, *Phys. Rev. Lett.* **2003**, *90*, 027402.

[34] M. T. Hill, M. Marell, E. S. P. Leong, B. Smalbrugge, Y. Zhu, M. Sun, P. J. van Veldhoven, E. J. Geluk, F. Karouta, Y.-S. Oei, R. Nötzel, C.-Z. Ning, M. K. Smit, *Opt. Express* **2009**, *17*, 11107.

[35] R. F. Oulton, V. J. Sorger, T. Zentgraf, R.-M. Ma, C. Gladden, L. Dai, G. Bartal, X. Zhang, *Nature* **2009**, *461*, 629.

[36] M. T. Hill, *J. Opt. Soc. Am. B* **2010**, *27*, B36.

[37] Y. Yin, T. Qiu, J. Li, P. K. Chu, *Nano Energy* **2012**, *1*, 25.

[38] K. Ding, C. Z. Ning, *Light: Sci. Appl.* **2012**, *1*, e20.

[39] P. Berini, I. De Leon, *Nat. Photonics* **2012**, *6*, 16.

[40] R. F. Oulton, *Nat. Photonics* **2012**, *6*, 219.

[41] R.-M. Ma, R. F. Oulton, V. J. Sorger, X. Zhang, *Laser Photonics Rev.* **2013**, *7*, 1.

[42] R. F. Oulton, *Mater. Today* **2012**, *15*, 26.

[43] M. C. Gather, *Nat. Photonics* **2012**, *6*, 708.

[44] M. T. Hill, in *Semiconductors and Semimetals*, Vol. *86* (Eds: J. J. Coleman, A. C. Bryce, C. Jagadish), Elsevier, Amsterdam, Holland **2012**, Ch. 9.

[45] M. Stockman, *Nat. Phys.* **2014**, *10*, 799.

[46] A. Yang, T. W. Odom, *IEEE Photonics J.* **2015**, *7*, 1.

[47] S. Gwo, C.-K. Shih, *Rep. Prog. Phys.* **2016**, *79*, 086501.

[48] J. S. T. Smalley, F. Vallini, Q. Gu, Y. Fainman, *Proc. IEEE* **2016**, *104*, 2323.

[49] Z. Wang, X. Meng, A. V. Kildishev, A. Boltasseva, V. M. Shalaev, *Laser Photonics Rev.* **2017**, *11*, 1700212.

[50] D. Wang, W. Wang, M. P. Knudson, G. C. Schatz, T. W. Odom, *Chem. Rev.* **2018**, *118*, 2865.

[51] V. I. Balykin, *Phys.-Usp.* **2018**, *61*, 846.

[52] Y.-H. Chou, C.-J. Chang, T.-R. Lin, T.-C. Lu, *Chin. Phys. B* **2018**, *27*, 114208.

[53] M. T. Hill, *Chin. Phys. B* **2018**, *27*, 114210.

[54] J. B. Khurgin, G. Sun, *Nat. Photonics* **2014**, *8*, 468.

[55] A. Kavokin, *Microcavities*, Oxford University Press, Oxford, UK **2007**.

[56] S. Strauf, F. Jahnke, *Laser Photonics Rev.* **2011**, *5*, 607.

[57] R.-M. Ma, R. F. Oulton, V. J. Sorger, G. Bartal, X. Zhang, *Nat. Mater.* **2011**, *10*, 110.

[58] M. Khajavikhan, A. Simic, M. Katz, J. H. Lee, B. Slutsky, A. Mizrahi, V. Lomakin, Y. Fainman, *Nature* **2012**, *482*, 204.

[59] J. Y. Suh, C. H. Kim, W. Zhou, M. D. Huntington, D. T. Co, M. R. Wasielewski, T. W. Odom, *Nano Lett.* **2012**, *12*, 5769.

[60] D. A. Genov, R. F. Oulton, G. Bartal, X. Zhang, *Phys. Rev. B* **2011**, *83*, 245312.

[61] X. Yu, Y. Yuan, J. Xu, K.-T. Yong, J. Qu, J. Song, *Laser Photonics Rev.* **2019**, *13*, 1800219.

[62] C. Schneider, A. Rahimi-Iman, N. Y. Kim, J. Fischer, I. G. Savenko, M. Amthor, M. Lermer, A. Wolf, L. Worschech, V. D. Kulakovskii, I. A. Shelykh, M. Kamp, S. Reitzenstein, A. Forchel, Y. Yamamoto, S. Hoefling, *Nature* **2013**, *497*, 348.

[63] S. Christopoulos, G. B. H. von Högersthal, A. J. D. Grundy, P. G. Lagoudakis, A. V. Kavokin, J. J. Baumberg, G. Christmann, R. Butté, E. Feltin, J.-F. Carlin, N. Grandjean, *Phys. Rev. Lett.* **2007**, *98*, 126405.

[64] J. Kasprzak, M. Richard, S. Kundermann, A. Baas, P. Jeambrun, J. M. J. Keeling, F. M. Marchetti, M. H. Szymańska, R. André, J. L. Staehli, V. Savona, P. B. Littlewood, B. Deveaud, L. S. Dang, *Nature* **2006**, *443*, 409.

[65] R. Balili, V. Hartwell, D. Snoke, L. Pfeiffer, K. West, *Science* **2007**, *316*, 1007.

[66] M. Ramezani, A. Halpin, A. I. Fernández-Domínguez, J. Feist, S. R.-K. Rodriguez, F. J. Garcia-Vidal, J. Gómez Rivas, *Optica* **2017**, *4*, 31.

[67] Y. Zhang, J. Wu, M. Aagesen, H. Liu, *J. Phys. D: Appl. Phys.* **2015**, *48*, 463001.

[68] G. Kewes, K. Herrmann, R. Rodríguez-Oliveros, A. Kuhlicke, O. Benson, K. Busch, *Phys. Rev. Lett.* **2017**, *118*, 237402.

[69] G. W. Ford, W. H. Weber, *Phys. Rep.* **1984**, *113*, 195.

[70] K. Joulain, R. Carminati, J.-P. Mulet, J.-J. Greffet, *Phys. Rev. B* **2003**, *68*, 245405.

[71] I. De Leon, P. Berini, *Nat. Photonics* **2010**, *4*, 382.

[72] A. Delga, J. Feist, J. Bravo-Abad, F. J. Garcia-Vidal, *Phys. Rev. Lett.* **2014**, *112*, 253601.

[73] A. V. Akimov, A. Mukherjee, C. L. Yu, D. E. Chang, A. S. Zibrov, P. R. Hemmer, H. Park, M. D. Lukin, *Nature* **2007**, *450*, 402.

[74] W. W. Chow, F. Jahnke, C. Gies, *Light: Sci. Appl.* **2014**, *3*, e201.

[75] G. Bjork, Y. Yamamoto, *IEEE J. Quantum Electron.* **1991**, *27*, 2386.

[76] G. Bjork, A. Karlsson, Y. Yamamoto, *Phys. Rev. A* **1994**, *50*, 1675.

[77] R.-M. Ma, R. F. Oulton, *Nat. Nanotechnol.* **2019**, *14*, 12.

[78] R. Brown, R. Twiss, *Nature* **1956**, *178*, 1046.

[79] P. B. Johnson, R. W. Christy, *Phys. Rev. B* **1972**, *6*, 4370.

[80] K. M. McPeak, S. V. Jayanti, S. J. P. Kress, S. Meyer, S. Iotti, A. Rossinelli, D. J. Norris, *ACS Photonics* **2015**, *2*, 326.

[81] J.-S. G. Bouillard, W. Dickson, D. P. O'Connor, G. A. Wurtz, A. V. Zayats, *Nano Lett.* **2012**, *12*, 1561.

[82] H. Yu, T. P. H. Sidiropoulos, W. Liu, C. Ronning, P. K. Petrov, S.-H. Oh, S. A. Maier, P. Jin, R. F. Oulton, *Adv. Opt. Mater.* **2017**, *5*, 1600856.

[83] Y.-J. Lu, J. Kim, H.-Y. Chen, C. Wu, N. Dabidian, C. E. Sanders, C.-Y. Wang, M.-Y. Lu, B.-H. Li, X. Qiu, W.-H. Chang, L.-J. Chen, G. Shvets, C.-K. Shih, S. Gwo, *Science* **2012**, *337*, 450.

[84] C.-W. Cheng, Y.-J. Liao, C.-Y. Liu, B.-H. Wu, S. S. Raja, C.-Y. Wang, X. Li, C.-K. Shih, L.-J. Chen, S. Gwo, *ACS Photonics* **2018**, *5*, 2624.

[85] Y. Wu, C. Zhang, N. M. Estakhri, Y. Zhao, J. Kim, M. Zhang, X.-X. Liu, G. K. Pribil, A. Alù, C.-K. Shih, X. Li, *Adv. Mater.* **2014**, *26*, 6106.

[86] E. D. Palik, *Handbook of Optical Constants of Solids*, Academic Press, San Diego, CA, USA **1998**.

[87] T. P. H. Sidiropoulos, R. Röder, S. Geburt, O. Hess, S. A. Maier, C. Ronning, R. F. Oulton, *Nat. Phys.* **2014**, *10*, 870.

[88] Y.-H. Chou, K.-B. Hong, Y.-C. Chung, C.-T. Chang, B.-T. Chou, T.-R. Lin, S. M. Arakelian, A. P. Alodjants, T.-C. Lu, *IEEE J. Sel. Top. Quantum Electron.* **2017**, *23*, 1.

[89] P. R. West, S. Ishii, G. V. Naik, N. K. Emani, V. M. Shalaev, A. Boltasseva, *Laser Photonics Rev.* **2010**, *4*, 795.

[90] G. V. Naik, V. M. Shalaev, A. Boltasseva, *Adv. Mater.* **2013**, *25*, 3264.

[91] G. V. Naik, J. Kim, A. Boltasseva, *Opt. Mater. Express* **2011**, *1*, 1090.

[92] G. V. Naik, J. L. Schroeder, X. Ni, A. V. Kildishev, T. D. Sands, A. Boltasseva, *Opt. Mater. Express* **2012**, *2*, 478.

[93] Y. G. Ma, X. Guo, X. Q. Wu, L. Dai, L. M. Tong, *Adv. Opt. Photonics* **2013**, *5*, 216.

[94] K. L. Shaklee, R. E. Nahory, R. F. Leheny, *J. Lumin.* **1973**, *7*, 284.

[95] Y.-J. Lu, C.-Y. Wang, J. Kim, H.-Y. Chen, M.-Y. Lu, Y.-C. Chen, W.-H. Chang, L.-J. Chen, M. I. Stockman, C.-K. Shih, S. Gwo, *Nano Lett.* **2014**, *14*, 4381.

[96] Y. Hou, P. Renwick, B. Liu, J. Bai, T. Wang, *Sci. Rep.* **2015**, *4*, 5014.

[97] T. Tao, T. Zhi, B. Liu, J. Dai, Z. Zhuang, Z. Xie, P. Chen, F. Ren, D. Chen, Y. Zheng, R. Zhang, *Adv. Funct. Mater.* **2017**, *27*, 1703198.

[98] Q. Zhang, R. Su, W. Du, X. Liu, L. Zhao, S. T. Ha, Q. Xiong, *Small Methods* **2017**, *1*, 1700163.

[99] S. D. Stranks, H. J. Snaith, *Nat. Nanotechnol.* **2015**, *10*, 391.

[100] B. R. Sutherland, E. H. Sargent, *Nat. Photonics* **2016**, *10*, 295.

[101] S. A. Veldhuis, P. P. Boix, N. Yantara, M. Li, T. C. Sum, N. Mathews, S. G. Mhaisalkar, *Adv. Mater.* **2016**, *28*, 6804.

[102] B. R. Sutherland, S. Hoogland, M. M. Adachi, P. Kanjanaboos, C. T. O. Wong, J. J. McDowell, J. Xu, O. Voznyy, Z. Ning, A. J. Houtepen, E. H. Sargent, *Adv. Mater.* **2015**, *27*, 53.

[103] M. J. H. Marell, B. Smalbrugge, E. J. Geluk, P. J. van Veldhoven, B. Barcones, B. Koopmans, R. Nötzel, M. K. Smit, M. T. Hill, *Opt. Express* **2011**, *19*, 15109.

[104] S. J. P. Kress, J. Cui, P. Rohner, D. K. Kim, F. V. Antolinez, K.-A. Zaininger, S. V. Jayanti, P. Richner, K. M. McPeak, D. Poulikakos, D. J. Norris, *Sci. Adv.* **2017**, *3*, e1700688.

[105] R. F. Oulton, V. J. Sorger, D. A. Genov, D. F. P. Pile, X. Zhang, *Nat. Photonics* **2008**, *2*, 496.

[106] S. Wang, B. Li, X.-Y. Wang, H.-Z. Chen, Y.-L. Wang, X.-W. Zhang, L. Dai, R.-M. Ma, *ACS Photonics* **2017**, *4*, 1355.

[107] S. Wang, H.-Z. Chen, R.-M. Ma, *Nano Lett.* **2018**, *18*, 7942.

[108] J. Homola, *Surface Plasmon Resonance Based Sensors*, Springer, Berlin/Heidelberg, Germany **2006**.

[109] R.-M. Ma, S. Ota, Y. Li, S. Yang, X. Zhang, *Nat. Nanotechnol.* **2014**, *9*, 600.

[110] X.-Y. Wang, Y.-L. Wang, S. Wang, B. Li, X.-W. Zhang, L. Dai, R.-M. Ma, *Nanophotonics* **2016**, *6*, 472.

[111] W. Zhu, T. Xu, H. Wang, C. Zhang, P. B. Deotare, A. Agrawal, H. J. Lezec, *Sci. Adv.* **2017**, *3*, e1700909.

[112] Q. Zhang, G. Li, X. Liu, F. Qian, Y. Li, T. C. Sum, C. M. Lieber, Q. Xiong, *Nat. Commun.* **2014**, *5*, 4953.

**ADVANCED
SCIENCE NEWS**

www.advancedsciencenews.com

**ADVANCED
OPTICAL
MATERIALS**

www.advopticalmat.de

[113] Y.-H. Chou, B.-T. Chou, C.-K. Chiang, Y.-Y. Lai, C.-T. Yang, H. Li, T.-R. Lin, C.-C. Lin, H.-C. Kuo, S.-C. Wang, T.-C. Lu, *ACS Nano* **2015**, *9*, 3978.

[114] B.-T. Chou, Y.-H. Chou, C.-K. Chiang, Y.-M. Wu, T.-R. Lin, S.-D. Lin, T.-C. Lu, *IEEE J. Sel. Top. Quantum Electron.* **2015**, *21*, 399.

[115] Y.-H. Chou, Y.-M. Wu, K.-B. Hong, B.-T. Chou, J.-H. Shih, Y.-C. Chung, P.-Y. Chen, T.-R. Lin, C.-C. Lin, S.-D. Lin, T.-C. Lu, *Nano Lett.* **2016**, *16*, 3179.

[116] B.-T. Chou, Y.-H. Chou, Y.-M. Wu, Y.-C. Chung, W.-J. Hsueh, S.-W. Lin, T.-C. Lu, T.-R. Lin, S.-D. Lin, *Sci. Rep.* **2016**, *6*, 19887.

[117] Y.-C. Chung, P.-J. Cheng, Y.-H. Chou, B.-T. Chou, K.-B. Hong, J.-H. Shih, S.-D. Lin, T.-C. Lu, T.-R. Lin, *Sci. Rep.* **2017**, *7*, 39813.

[118] J. Lu, M. Jiang, M. Wei, C. Xu, S. Wang, Z. Zhu, F. Qin, Z. Shi, C. Pan, *ACS Photonics* **2017**, *4*, 2419.

[119] S. Liu, B. Sheng, X. Wang, D. Dong, P. Wang, Z. Chen, T. Wang, X. Rong, D. Li, L. Yang, S. Liu, M. Li, J. Zhang, W. Ge, K. Shi, Y. Tong, B. Shen, *Appl. Phys. Lett.* **2018**, *112*, 231904.

[120] J. Ho, J. Tatebayashi, S. Sergent, C. F. Fong, S. Iwamoto, Y. Arakawa, *ACS Photonics* **2015**, *2*, 165.

[121] H. Yu, K. Ren, Q. Wu, J. Wang, J. Lin, Z. Wang, J. Xu, R. F. Oulton, S. Qu, P. Jin, *Nanoscale* **2016**, *8*, 19536.

[122] J. Ho, J. Tatebayashi, S. Sergent, C. F. Fong, Y. Ota, S. Iwamoto, Y. Arakawa, *Nano Lett.* **2016**, *16*, 2845.

[123] C.-J. Lee, H. Yeh, F. Cheng, P.-H. Su, T.-H. Her, Y.-C. Chen, C.-Y. Wang, S. Gwo, S. R. Bank, C.-K. Shih, W.-H. Chang, *ACS Photonics* **2017**, *4*, 1431.

[124] A. Tamada, Y. Ota, K. Kuruma, J. Ho, K. Watanabe, S. Iwamoto, Y. Arakawa, *Jpn. J. Appl. Phys.* **2017**, *56*, 102001.

[125] H. Chen, S. Wang, R. Ma, *IEEE J. Quantum Electron.* **2018**, *54*, 1.

[126] C.-Y. Wu, C.-T. Kuo, C.-Y. Wang, C.-L. He, M.-H. Lin, H. Ahn, S. Gwo, *Nano Lett.* **2011**, *11*, 4256.

[127] N. Liu, A. Gocalinska, J. Justice, F. Gity, I. Povey, B. McCarthy, M. Pemble, E. Pelucchi, H. Wei, C. Silien, H. Xu, B. Corbett, *Nano Lett.* **2016**, *16*, 7822.

[128] Q. Zhang, Q. Shang, J. Shi, J. Chen, R. Wang, Y. Mi, W. Du, C. Shen, R. Ma, X. Qiu, X. Liu, T. C. Sum, *ACS Photonics* **2017**, *4*, 2789.

[129] Z. Wu, J. Chen, Y. Mi, X. Sui, S. Zhang, W. Du, R. Wang, J. Shi, X. Wu, X. Qiu, Z. Qin, Q. Zhang, X. Liu, *Adv. Opt. Mater.* **2018**, *6*, 1800674.

[130] A. M. Lakhani, M.-k. Kim, E. K. Lau, M. C. Wu, *Opt. Express* **2011**, *19*, 18237.

[131] P.-J. Cheng, Z.-T. Huang, J.-H. Li, B.-T. Chou, Y.-H. Chou, W.-C. Lo, K.-P. Chen, T.-C. Lu, T.-R. Lin, *ACS Photonics* **2018**, *5*, 2638.

[132] X. Q. Wu, Y. Xiao, C. Meng, X. N. Zhang, S. L. Yu, Y. P. Wang, C. X. Yang, X. Guo, C. Z. Ning, L. M. Tong, *Nano Lett.* **2013**, *13*, 5654.

[133] S. Raza, S. I. Bozhevolnyi, M. Wubs, N. A. Mortensen, *J. Phys.: Condens. Matter* **2015**, *27*, 183204.

[134] M. A. Noginov, G. Zhu, A. M. Belgrave, R. Bakker, V. M. Shalaev, E. E. Narimanov, S. Stout, E. Herz, T. Suteewong, U. Wiesner, *Nature* **2009**, *460*, 1110.

[135] S.-Y. Liu, J. Li, F. Zhou, L. Gan, Z.-Y. Li, *Opt. Lett.* **2011**, *36*, 1296.

[136] X. Meng, A. V. Kildishev, K. Fujita, K. Tanaka, V. M. Shalaev, *Nano Lett.* **2013**, *13*, 4106.

[137] J. Cuerda, F. J. García-Vidal, J. Bravo-Abad, *ACS Photonics* **2016**, *3*, 1952.

[138] E. I. Galanzha, R. Weingold, D. A. Nedosekin, M. Sarimollaoglu, J. Nolan, W. Harrington, A. S. Kuchyanov, R. G. Parkhomenko, F. Watanabe, Z. Nima, A. S. Biris, A. I. Plekhanov, M. I. Stockman, V. P. Zharov, *Nat. Commun.* **2017**, *8*, 15528.

[139] C. Alix-Panabieres, K. Pantel, *Nat. Mater.* **2017**, *16*, 790.

[140] N. I. Zheludev, S. L. Prosvirnin, N. Papasimakis, V. A. Fedotov, *Nat. Photonics* **2008**, *2*, 351.

[141] F. van Beijnum, P. J. van Veldhoven, E. J. Geluk, M. J. A. de Dood, G. W. 't Hooft, M. P. van Exter, *Phys. Rev. Lett.* **2013**, *110*, 206802.

[142] W. Zhou, M. Dridi, J. Y. Suh, C. H. Kim, D. T. Co, M. R. Wasielewski, G. C. Schatz, T. W. Odom, *Nat. Nanotechnol.* **2013**, *8*, 506.

[143] A. H. Schokker, A. F. Koenderink, *Phys. Rev. B* **2014**, *90*, 155452.

[144] X. Meng, J. Liu, A. V. Kildishev, V. M. Shalaev, *Laser Photonics Rev.* **2014**, *8*, 896.

[145] A. Yang, Z. Li, M. P. Knudson, A. J. Hryn, W. Wang, K. Aydin, T. W. Odom, *ACS Nano* **2015**, *9*, 11582.

[146] C. Zhang, Y. Lu, Y. Ni, M. Li, L. Mao, C. Liu, D. Zhang, H. Ming, P. Wang, *Nano Lett.* **2015**, *15*, 1382.

[147] A. Yang, T. B. Hoang, M. Dridi, C. Deeb, M. H. Mikkelsen, G. C. Schatz, T. W. Odom, *Nat. Commun.* **2015**, *6*, 6939.

[148] H.-Y. Wu, L. Liu, M. Lu, B. T. Cunningham, *Adv. Opt. Mater.* **2016**, *4*, 708.

[149] V. T. Tenner, M. J. A. de Dood, M. P. van Exter, *ACS Photonics* **2016**, *3*, 942.

[150] A. H. Schokker, A. F. Koenderink, *Optica* **2016**, *3*, 686.

[151] R. Chandrasekar, Z. Wang, X. Meng, S. I. Azzam, M. Y. Shalaginov, A. Lagutchev, Y. L. Kim, A. Wei, A. V. Kildishev, A. Boltasseva, V. M. Shalaev, *ACS Photonics* **2017**, *4*, 674.

[152] D. Wang, A. Yang, W. Wang, Y. Hua, R. D. Schaller, G. C. Schatz, T. W. Odom, *Nat. Nanotechnol.* **2017**, *12*, 889.

[153] T. B. Hoang, G. M. Akselrod, A. Yang, T. W. Odom, M. H. Mikkelsen, *Nano Lett.* **2017**, *17*, 6690.

[154] S.-H. Kim, W. S. Han, T.-Y. Jeong, H.-R. Lee, H. Jeong, D. Lee, S.-B. Shim, D.-S. Kim, K. J. Ahn, K.-J. Yee, *Sci. Rep.* **2017**, *7*, 7907.

[155] D. Wang, M. R. Bourgeois, W.-K. Lee, R. Li, D. Trivedi, M. P. Knudson, W. Wang, G. C. Schatz, T. W. Odom, *Nano Lett.* **2018**, *18*, 4549.

[156] K. S. Daskalakis, A. I. Väkeväinen, J.-P. Martikainen, T. K. Hakala, P. Törmä, *Nano Lett.* **2018**, *18*, 2658.

[157] N. E. Nefedkin, A. A. Zyablovsky, E. S. Andrianov, A. A. Pukhov, A. P. Vinogradov, *ACS Photonics* **2018**, *5*, 3031.

[158] C. Deeb, Z. Guo, A. Yang, L. Huang, T. W. Odom, *Nano Lett.* **2018**, *18*, 1454.

[159] F. Cao, L. Niu, J. Tong, S. Li, A. Hayat, M. Wang, T. Zhai, X. Zhang, *Opt. Express* **2018**, *26*, 13383.

[160] K.-C. Shen, C.-T. Ku, C. Hsieh, H.-C. Kuo, Y.-J. Cheng, D. P. Tsai, *Adv. Mater.* **2018**, *30*, 1706918.

[161] V. T. Tenner, M. J. A. de Dood, M. P. van Exter, *Opt. Lett.* **2018**, *43*, 166.

[162] H. T. Rekola, T. K. Hakala, P. Törmä, *ACS Photonics* **2018**, *5*, 1822.

[163] C. Symonds, A. Lemaître, P. Senellart, M. H. Jomaa, S. Aberra Guebrou, E. Homeyer, G. Brucoli, J. Bellessa, *Appl. Phys. Lett.* **2012**, *100*, 121122.

[164] C. Symonds, G. Lheureux, J. P. Hugonin, J. J. Greffet, J. Laverdant, G. Brucoli, A. Lemaitre, P. Senellart, J. Bellessa, *Nano Lett.* **2013**, *13*, 3179.

[165] G. Lheureux, S. Azzini, C. Symonds, P. Senellart, A. Lemaître, C. Sauvan, J.-P. Hugonin, J.-J. Greffet, J. Bellessa, *ACS Photonics* **2015**, *2*, 842.

[166] R. A. Flynn, C. S. Kim, I. Vurgaftman, M. Kim, J. R. Meyer, A. J. Mäkinen, K. Bussmann, L. Cheng, F.-S. Choa, J. P. Long, *Opt. Express* **2011**, *19*, 8954.

[167] E. K. Keshmarzi, R. N. Tait, P. Berini, *Nanoscale* **2018**, *10*, 5914.

[168] D. Zhang, S. Chen, Y. Huang, Z. Zhang, Y. Wang, D. Ma, *J. Appl. Phys.* **2015**, *117*, 023106.

[169] Q. Qiao, C.-X. Shan, J. Zheng, H. Zhu, S.-F. Yu, B.-H. Li, Y. Jia, D.-Z. Shen, *Nanoscale* **2012**, *5*, 513.

[170] A. H. Schokker, A. F. Koenderink, *ACS Photonics* **2015**, *2*, 1289.

[171] S. Ning, Z. Wu, H. Dong, L. Ma, B. Jiao, L. Ding, L. Ding, F. Zhang, *Org. Electron.* **2016**, *30*, 165.

[172] T. Zhai, Z. Xu, X. Wu, Y. Wang, F. Liu, X. Zhang, *Opt. Express* **2016**, *24*, 437.

[173] Z. Wang, X. Meng, S. H. Choi, S. Knitter, Y. L. Kim, H. Cao, V. M. Shalaev, A. Boltasseva, *Nano Lett.* **2016**, *16*, 2471.

[174] X. Huang, P. Zhang, E. Lin, P. Wang, M. Mei, Q. Huang, J. Jiao, Q. Zhao, *Appl. Phys. A* **2017**, *123*, 605.

[175] M.-K. Seo, S.-H. Kwon, H.-S. Ee, H.-G. Park, *Nano Lett.* **2009**, *9*, 4078.

[176] V. Apalkov, M. I. Stockman, *Light: Sci. Appl.* **2014**, *3*, e191.

[177] C. Rupasinghe, I. D. Rukhlenko, M. Premaratne, *ACS Nano* **2014**, *8*, 2431.

[178] Y. Y. Huo, T. Q. Jia, Y. Zhang, H. Zhao, S. A. Zhang, D. H. Feng, Z. R. Sun, *Appl. Phys. Lett.* **2014**, *104*, 113104.

[179] T. Pickering, J. M. Hamm, A. F. Page, S. Wuestner, O. Hess, *Nat. Commun.* **2014**, *5*, 4972.

[180] K. Liu, V. J. Sorger, *Opt. Mater. Express* **2015**, *5*, 1910.

[181] S. Wuestner, J. M. Hamm, A. Pusch, O. Hess, *Laser Photonics Rev.* **2015**, *9*, 256.

[182] H. P. Paudel, V. Apalkov, M. I. Stockman, *Phys. Rev. B* **2016**, *93*, 155105.

[183] C. Jayasekara, M. Premaratne, S. D. Gunapala, M. I. Stockman, *J. Appl. Phys.* **2016**, *119*, 133101.

[184] C. Zheng, T. Jia, H. Zhao, S. Zhang, D. Feng, Z. Sun, *J. Phys. D: Appl. Phys.* **2016**, *49*, 015101.

[185] B. Liu, W. Zhu, S. D. Gunapala, M. I. Stockman, M. Premaratne, *ACS Nano* **2017**, *11*, 12573.

[186] L. Wang, J. Qu, J. Song, J. Xian, *Plasmonics* **2017**, *12*, 1145.

[187] Y.-H. Chou, K.-B. Hong, C.-T. Chang, T.-C. Chang, Z.-T. Huang, P.-J. Cheng, J.-H. Yang, M.-H. Lin, T.-R. Lin, K.-P. Chen, S. Gwo, T.-C. Lu, *Nano Lett.* **2018**, *18*, 747.

[188] I. O. Zolotovskii, Y. S. Dadoenkova, S. G. Moiseev, A. S. Kadochkin, V. V. Svetukhin, A. A. Fotiadi, *Phys. Rev. A* **2018**, *97*, 053828.

[189] Y. Ye, F. Liu, K. Cui, X. Feng, W. Zhang, Y. Huang, *Opt. Express* **2018**, *26*, 31402.

[190] S.-H. Kwon, J.-H. Kang, C. Seassal, S.-K. Kim, P. Regreny, Y.-H. Lee, C. M. Lieber, H.-G. Park, *Nano Lett.* **2010**, *10*, 3679.

[191] K. Yu, A. Lakhani, M. C. Wu, *Opt. Express* **2010**, *18*, 8790.

[192] A. M. Lakhani, K. Yu, M. C. Wu, *Semicond. Sci. Technol.* **2011**, *26*, 014013.

[193] S. Kwon, J. Kang, S. Kim, H. Park, *IEEE J. Quantum Electron.* **2011**, *47*, 1346.

[194] J.-H. Kang, Y.-S. No, S.-H. Kwon, H.-G. Park, *Opt. Lett.* **2011**, *36*, 2011.

[195] E. Cubukcu, N. Yu, E. J. Smythe, L. Diehl, K. B. Crozier, F. Capasso, *IEEE J. Sel. Top. Quantum Electron.* **2008**, *14*, 1448.

[196] N. Yu, Q. Wang, F. Capasso, *Laser Photonics Rev.* **2012**, *6*, 24.

[197] P. Fan, C. Colombo, K. C. Y. Huang, P. Krogstrup, J. Nygård, A. Fontcuberta i Morral, M. L. Brongersma, *Nano Lett.* **2012**, *12*, 4943.

[198] Y.-S. No, J.-H. Choi, H.-S. Ee, M.-S. Hwang, K.-Y. Jeong, E.-K. Lee, M.-K. Seo, S.-H. Kwon, H.-G. Park, *Nano Lett.* **2013**, *13*, 772.

[199] Z. Chen, B. Lai, J. Zhang, G. Wang, S. Chu, *Nanotechnology* **2014**, *25*, 295203.

[200] Y. J. Li, Y. Lv, C.-L. Zou, W. Zhang, J. Yao, Y. S. Zhao, *J. Am. Chem. Soc.* **2016**, *138*, 2122.

[201] P. Molina, E. Yraola, M. O. Ramírez, C. Tserkezis, J. L. Plaza, J. Aizpurua, J. Bravo-Abad, L. E. Bausá, *Nano Lett.* **2016**, *16*, 895.

[202] D. Hernández-Pinilla, P. Molina, C. de las Heras, J. Bravo-Abad, L. E. Bausá, M. O. Ramírez, *ACS Photonics* **2018**, *5*, 406.

[203] E. Ozbay, *Science* **2006**, *311*, 189.

[204] X. Guo, Y. G. Ma, Y. P. Wang, L. M. Tong, *Laser Photonics Rev.* **2013**, *7*, 855.

[205] S. Wang, X.-Y. Wang, B. Li, H.-Z. Chen, Y.-L. Wang, L. Dai, R. F. Oulton, R.-M. Ma, *Nat. Commun.* **2017**, *8*, 1889.

[206] F. Wang, Y. R. Shen, *Phys. Rev. Lett.* **2006**, *97*, 206806.

[207] M. Jablan, H. Buljan, M. Soljačić, *Phys. Rev. B* **2009**, *80*, 245435.

[208] J. Chen, M. Badioli, P. Alonso-González, S. Thongrattanasiri, F. Huth, J. Osmond, M. Spasenović, A. Centeno, A. Pesquera, P. Godignon, A. Z. Elorza, N. Camara, F. J. G. de Abajo, R. Hillenbrand, F. H. L. Koppens, *Nature* **2012**, *487*, 77.

[209] F. J. García de Abajo, *ACS Photonics* **2014**, *1*, 135.

[210] Z. Fei, M. E. Scott, D. J. Gosztola, J. J. Foley, J. Yan, D. G. Mandrus, H. Wen, P. Zhou, D. W. Zhang, Y. Sun, J. R. Guest, S. K. Gray, W. Bao, G. P. Wiederrecht, X. Xu, *Phys. Rev. B* **2016**, *94*, 081402.

[211] D. N. Basov, M. M. Fogler, F. J. G. de Abajo, *Science* **2016**, *354*, aag1992.

[212] I. Khrapach, F. Withers, T. H. Bointon, D. K. Polyushkin, W. L. Barnes, S. Russo, M. F. Craciun, *Adv. Mater.* **2012**, *24*, 2844.

[213] Z. Shi, X. Hong, H. A. Bechtel, B. Zeng, M. C. Martin, K. Watanabe, T. Taniguchi, Y.-R. Shen, F. Wang, *Nat. Photonics* **2015**, *9*, 515.

[214] T. K. Hakala, A. J. Moilanen, A. I. Väkeväinen, R. Guo, J.-P. Martikainen, K. S. Daskalakis, H. T. Rekola, A. Julku, P. Törmä, *Nat. Phys.* **2018**, *14*, 739.